DEVELOPMENT OF A NUMERICAL MODEL OF SYNGAS EXPANSION IN A GAS TURBINE UTILIZING MUI BASIN COAL

AGATHA MBENI MUINDE

MASTER OF SCIENCE
(Mechanical Engineering)

JOMO KENYATTA UNIVERSITY OF AGRICULTURE AND TECHNOLOGY

2022

Development of a Numerical Model of Syngas Expansion in a Gas Turbine Utilizing Mui Basin Coal

Agatha Mbeni Muinde

A Thesis Submitted in Partial Fulfilment of the Requirements for the Degree of Master of Science in Mechanical Engineering of the Jomo Kenyatta University of Agriculture and Technology

2022

DECLARATION

This thesis is my original work and has not been presented for a degree in any other university.

Signature..... Date.....

Agatha Mbeni Muinde

This thesis has been submitted for examination with our approval as university supervisors:

Signature..... Date.....

Dr. (Eng) Hiram M. Ndiritu, PhD

JKUAT, Kenya

Signature..... Date.....

Dr. Benson B. Gathitu, PhD

JKUAT, Kenya

DEDICATION

To Christine, Solomon and Olive; You can do all things through Christ who strengthens you (Phil 4:13).

ACKNOWLEDGMENT

Thanks be to God the Almighty, first and foremost, for giving me the opportunity to do this research. May I sincerely thank my supervisors Dr. (Eng.) Hiram Ndiritu and Dr. Benson Gathitu who guided and supported me throughout the research period. I am also very grateful to the Government of Kenya through National Research Fund for the grant and JKUAT for offering me a scholarship to do MSc. in Mechanical Engineering.

Finally, I want to extend my gratitude to the staff members, technologists and technicians of mechanical engineering department for their assistance during this period.

TABLE OF CONTENTS

LIST OF TABLES

LIST OF FIGURES

LIST OF ABBREVIATIONS

P	Static pressure
T	Temperature
K	Kelvin
g	Acceleration due to gravity
h	Elevation
R	Gas constant
M	Molecular mass
MW	Megawatts
TIT	Turbine Inlet Temperature
CFD	Computational fluids dynamics
SST	Shear Stress Turbulence
HHV	Higher heating value
LHV	Lower heating value
H_2	Hydrogen
CO	Carbon monoxide
NOx	Oxides of nitrogen
PPM	Parts per million
RPM	Revolutions per minute
r	Rotor
s	Stator
Syngas	Synthesis Gas

LIST OF SYMBOLS

α	Lean Angle (degree)
β	Sweep Angle (degree)
C_p	Specific Heat Capacity (kJ/kgK)
η	Efficiency
γ	Adiabatic Constant
$\dot{H}$	Heat Input (J/mm)
λ	Heat Conductivity (W/mK)
μ	Dynamic Viscosity (kg/ms)
∇	Divergence Operator
∂	Partial Differential Operator
ρ	Density (kg/m^3)
$\sigma_k, \sigma_\epsilon$	Closure Coefficients
T_e	Turbine Exit Temperature (K)
T_i	Turbine Inlet Temperature (K)
x, y, z	Co-ordinate axes for plots

ABSTRACT

The global energy demand has been increasing over the years and is still expected to increase by 25% in 2040. The rise in demand is being accelerated by economic growth and industrialization of developing countries in Africa and also due to the projected global population increase to 9 billion by 2040. Fossil fuels have been the major source of global energy. By the end of 20^{th} century they accounted for 85% of the total energy consumed. Combustion of the fossil fuels to run machines productes greenhouse gases. Hence there is need for clean, cheap and reliable source of energy to meet the rise in demand. Coal is a cheap, dirty source of energy that is currently used to generate 41.5% of the world electricity and to meet 26.5% of global primary energy needs. Technologies have been developed to reduce emissions from coal power plants such as flue gas scrabing, clean coal, and the use of alternative fuel like natural gas. Clean coal technologies include; pressurized fluidized bed combustion, Integrated Gasification Combined Cycle (IGCC),carbon capture and storage. Fluidized bed combustion have reduced emissions but it is difficult to fluidize fine particles while further studies are still being done on coal gasification. Kenya discovered 400 million tonnes of coal ranging from lignite to sub-bituminous having calorific values between 16 and 27 MJ/kg in Mui Basin Kitui county. Construction of coal power plants is underway in Kenya and hence studies are needed on clean and efficient utilization of the available resource. Research on gasification of the coal to produce syngas has already been done. The current research is on simulation of syngas combustion gases expansion in a gas turbine rotor. The main objective of this study was to develop a numerical model for simulation of syngas expansion in a gas turbine utilizing mui basin coal. To achieve this a gas turbine rotor model was developed and Computational fluid dynamics (CFD) software was used to simulate the flow. Syngas used was from gasification of lignite coal while simulation fluid was combustion gases of hydrogen and carbon monoxide. The rotational speed, pressure ratio and inlet temperature of turbine were varied while performance of the rotor was being recorded. Results of this study showed that efficiency increased with increase in pressure ratio, rotational speed and inlet temperature up to maximum then started to decrease. Power was directly proportional to temperature and rotational speed while it was inversely to pressure ratio. The maximum efficiency of 92.7% and power of 2.5 kW was attained at rotational speed of 10,000 rpm, pressure ratio of 10, and inlet temperature of 900 K.

CHAPTER ONE

INTRODUCTION

1.1 Background

The global energy demand has been on a steady rise and this increase is expected to be more rapid as economies grow. The energy demand is expected to rise by 3.5% per year to 2040. This is due to the projected global growth of population to 9 billion 2040 and also due to the expected icrease in Gross domestic product (GDP)(Spencer, 2019). Clean, efficient, affordable and reliable energy services is crucial for global prosperity (AGECC, 2010).

Energy is a priority in Kenya so as to achieve Vision 2030 which aims at making the country a middle income economy and start new industries and offer citizens quality life (Boulle, 2019). As at 2015 the electricity demand was at 1,600 MW and it was projected be 10,000 MW by 2035 (Lahmeyer International, 2016). The rise in demand will be as a result of population growth and increased connectivity (dubbed last mile connection) as the government of Kenya seeks have 100% access to power by 2023 (of Kenya, 2018).

Developing economies like Kenya need modern energy services to increase productivity and promote economic growth (AGECC, 2010). Gas turbines are preferred for power generation globally due to their high cycle efficiency, less installation time and reduced NO_x and CO_2 emissions (Bhargava, Bianchi, De Pascale, Negri di Montenegro, & Peretto, 2007). The current gas turbine efficiency is 40% and advancement in technologies are expected to make it 75% (T. K. Ibrahim, Mohammed, Al Doori, Al-Sammarraie, & Basrawi, 2019).

1.2 Gas Turbine Fuels

When gas turbines started being used a variety of fuels were used to fire them. The heating value of the fuel affects flow rate and blade area. Gas turbines can be fired with a variety of fuels; solid, liquid and even gas. The diversity in fuels make gas turbines useful for many purposes. The use of syngas from biomass, municipal waste and coal is making the gas turbine useful in recycling waste and hence being more environmental friendly (Indrawan, Kumar, Moliere, Sallam, & Huhnke, 2020).

Fossil fuels which include liquid fuels, natural gas and coal currently dominate the global energy supply by over 84% (BP, 2020). The calorific value of natural gas, crude oil and coal is 50 GJ/tonne, 45 GJ/tonne and 30 GJ/tonne respectively (Self, Reddy, & Rosen, 2012). Petroleum based fuels are still the world largest source of energy at 36% (Spencer, 2019). But the rising oil prices have led to the use of energy efficient technologies like hybrid and electric cars resulting in high demand for electricity. Natural gas use continues to rise at the rate of 2% per year, due to the abundance in supply and the less emission during use (BP, 2020).

Combustion of coal in gas turbine started as early as the invention of the industrial gas turbine. Since then, coal continues to be the largest single fuel for world's electricity at 36% and for global primary energy needs at 27% (BP, 2020). Coal is the main source of energy in India and Greater Southeast Asia and the consumption grows by 3% per year and it is expected to account for 35% of world's demand by 2050 (Energy Information Administration, 2022). The modern Rankine cycle power plants use coal as a source of heat to produce power and have an efficiency of 42% and the older ones 35%-40% (I. B. Matveev, 2011). Coal is the most carbon intense fossil fuel and has the lowest calorific value, hence producing the highest CO_2 emission per unit of thermal energy (Self et al., 2012). Low efficiency and high level of pollution in coal-fired power plants has led to alternative uses of coal such as gasified syngas in gas turbines (I. B. Matveev, 2011). Coal is converted to syngas and used in gas

turbines for power production.

In 2007 Kenya discovered 400 million tonnes of coal reserves in the Mui Basin (Boulle, 2019). After analysis the coal ranged in ranking from lignite to sub-bituminous with calorific values ranging between 16 and 27 MJ/kg in Mui Basin Kitui county (and Petroleum, 2015), (Nzove, 2021). The Kenyan government has proposed construction of two coal power plant 1050 MW at Lamu and another 960 MW in Kitui near the Mui Basin. Lamu plant will use pulverized coal from South Africa and later the Mui Basin coal when mining will start (Power & Limited, 2016). The Lamu coal power plant construction has stalled due to pollution concerns from the residents(Bwana, 2021).

The high carbon emissions from the combustion of coal have led to development of flue gas scraping and clean coal technologie which remove carbon dioxide. In the flue gas scraping the flue gases are passed through processes that remove the particulate matter like filters and then the carbon is absorbed through some solutions. Clean coal technologies include; pressurized fluidized bed combustion, Integrated Gasification Combined Cycle (IGCC), carbon capture and storage (Self et al., 2012). In gasification the coal is pre-combusted to produce syngas and the carbon dioxide is captured, the remaining gas is combusted to produce energy. The use of integrated gasification combined cycle is being used in trial stages but it is very promising (Spliethoff, 2010).

1.3 Problem Statement

Energy is a key driver of global economic development and it is mainly utilized in transport, industry and households. The industrial sector has been the leading consumer of energy for a long time since 1971. The residential and commercial buildings consume 31% of the total delivered energy consumed worldwide as at 2014 (IEA, 2015). The residential energy consumption is estimated to increase at an

annual average of 1.4% while the commercial one is estimated to increase at an annual average rate of 1.6% from 2012 to 2040 (IEA, 2015). As at December 2019 the installed capacity of power in Kenya was at 2,929 MW. The energy mix comprises of; hydro 29%, geothermal 28%, thermal 26%, Wind 11%, Solar 3% and Bioenergy 3% (Takase, Kipkoech, & Essandoh, 2021). Hydro power forms the highest percentage yet it is unreliable due to low water levels in the dams during dry season. Thermal power plants are used as back up power during the peak hours and dry seasons hence the high cost of fuel is reflected as fuel levy in electricity bill. The cost of drilling one geothermal well is on average 3 million US dollars meaning that despite their contribution to the energy mix costs for projects are 13 US cents per kWh. Coal as a source of power generation is yet to be fully explored in Kenya (Ngugi, 2012).

Coal generates over 40% of the world electricity but its utilization has been affected by its impact on environment(Self et al., 2012). Coal combustion causes the highest emissions when compared to other fossil fuels. Clean coal technologies like pulverized coal, flue gas treatment and fluidized bed combustion have reduced emissions but it is difficult to fluidize fine particles (Jamshidi & Mazzei, 2018). Coal gasification reduces emission of pollutants to the environment and is one mechanism of clean coal utilization that require further study(Hagos, Aziz, & Sulaiman, 2014).

Most of the existing gas turbines are manufactured specifically to burn standard fuels like natural gas and light diesel fuel (Joo, Kim, Park, & Seo, 2016) (Xuelei, Songling, Haiping, & Lanxin, 2010). Liu *et al.* (Liu & Weng, 2009) studied the effects of low heating value fuel on the operations of micro-gas turbine using Matlab/Simulink software. The findings were that adjusting compression ratio and turbine inlet temperature lowered power output and efficiency. Joo *et al.* (Joo et al., 2016) studied the performance analysis of gas turbine for large-scale IGCC power plant using GateCycle software. The findings were that when running a natural gas turbine using syngas there was a limit in the power output at 230 MW and it was below capacity of pulverised coal which was 1000 MW. Research is needed to determine

maximum power and efficiency of a syngas gas turbine which can be used when deciding on the proposed Kitui and Lamu coal power plants.

1.4 Objectives

The main objective of this research was to develop a numerical model for simulation of syngas expansion in a gas turbine utilizing Mui basin lignite coal. This was achieved via the following specific objectives;

- To develop a validated model for performance simulation of syngas combustion gases expansion in a gas turbine
- To evaluate the influence of pressure ratio on syngas gas turbine efficiency.
- To evaluate rotational speed and inlet temperature variation on performance of the turbine

1.5 Justification

Energy is essential for the growth of the economy all over the world. In the vision 2030 Kenya requires energy for its social and economical transformation (Republic of Kenya, 2014). Carbon taxes had been imposed as of mid 2015 covering 12% of the global energy related CO_2 emissions the aim is to have them at zero by 2060 (Rogelj, Smith, & Yu, 2021). These taxes have made Kenya to intensify and expand utilization of sustainable energy sources that have low carbon emissions.

The discovery of coal in Kenya led to construct plans of a pulverized coal power plant which has been halted due to emission concerns (Bwana, 2021). Combustion of coal produces large quantities of carbon emissions hence gasifications helps to reduce them by incorporating capture and storage technology. This research sought to develop a clean method of producing power using coal. A gas turbine rotor model

was developed and syngas combustion gases expanded though it to determine the power and efficiency of the system.

1.6 Outline of Thesis

This thesis has five chapters. The current chapter is introduction to the research which presents a general overview of the existing problem related to energy crisis and coal use. Existing literature review on coal gasification, gas turbine advancements and syngas turbine rotor design is highlighted in Chapter 2. Modeling of axial flow gas turbine rotor, governing equations and CFD modeling are outlined in Chapter 3. Results of influence speed, temperature and pressure ratio on the efficiency, power and torque are discussed in Chapter 4. Chapter 5 has conclusions derived from the determined performance parameters and recommendations for further work on syngas turbine optimization.

CHAPTER TWO

LITERATURE REVIEW

2.1 Overview

A rise in global energy demand has led to increased utilization of fossil fuels such as coal and petroleum. This has in turn led to the search for alternative and cleaner sources of energy. Coal emissions has led to research on gasification to generate syngas for use in gas turbines to produce power efficiently. This chapter presents historical development of gas turbines including concepts and theories that have been explored in a bid to improve their performance, findings of previous researchers and the gaps from their work that require further interventions.

2.2 History of Gas turbines

The first gas turbine was patented by John Barber in 1791 and it had most of of modern day gas turbines elements (Bathie, 1996). Barber's invention shown in Figure 2.1, opened way for other inventors who made efforts to improve the gas turbine. He designed it to power a horseless carriage. The challenge was that the gas turbine could not generate sufficient power to run its components and other systems (Bathie, 1996), (Meher-Homji, 2000).

The first industrial gas turbine used for power generation was built by Brown Boveri in 1939. It had a capacity of 4 MW and was used for running an emergency power station in Neuchâtel, Switzerland (ASME, 2007). The challenge was efficiency of 18% caused by low inlet temperature of 773 K.

The gas turbines performance is continuously being improved to increase their

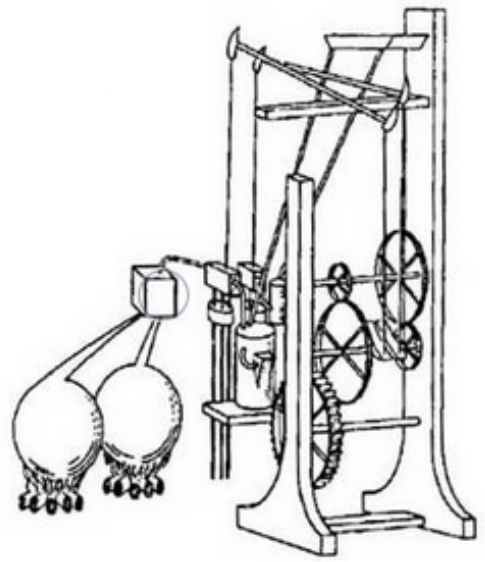

Figure 2.1: John barber's gas turbine (Bathie, 1996)

efficiency, power output, reduce their emissions, reduce fuel consumption and increase the life cycle. Thermal efficiency and blade lifespan can be increased by increased inlet temperature, blade cooling and an optimum blade clearance. These factors are explored in the following section.

2.3 Types of Turbines

Gas turbines are classified according to their function, cycle and also configuration. The major types according to function are: Jet engines; they are used to produce thrust force through the exhaust gas, auxiliar power units; are small gas turbines used to run larger machines, industrial gas turbines for electricity generation; they are used to generate electricity and to recover residual energy and they have a thermal efficiency of 30%, industrial gas turbines for mechanical drive; they are used in conjunction with other machines, Turboshaft engine; they are used to drive compressors and they are used in most modern helicopters, vehicle turbo chargers; they are small electricity generators from burning gaseous and liquid fuels to create high speed rotation with an efficiency of 25 to 35% (Almarzooq, 2014). The

classification according to cycle are; open cycle in which exhaust gas is released to the environment, and closed cycle in which the exhaust gas is passed through a heat recovery system where steam is generated and used to run a steam turbine hence a higher efficiency (Weston, 2000). The classification according to configuration has two types namely; radial flow turbines in which the flow is along the radius and axial flow turbines in which flow is along the axis of rotation (Gorla & Khan, 2003).

2.3.1 Axial Flow Turbines

The axial flow turbine can have one or more stages, each consisting of a stationary nozzle and a rotor. The turbine extracts kinetic energy of the expanding gases from the burner and converts it into shaft power to drive the compressor and different engine accessories depending on the application. Blade notation for ideal axial flow turbine is shown in Figure 2.2. A key feature of these turbines is that the fluid enters at the leading edge and leaves at the trailing edge at an angle tangent to the camber line (as shown in the Figure 2.2) (Guédez, 2011). The axial flow turbines are preferred to radial flow ones because they can be used for incompressible fluids, have higher efficiency for high power range above 5 MW and they have a high work factor hence a lower fuel consumption and less turbine noise (Binder, Carbonneau, & Chassaing, 2008).

Axial flow turbines are divided into reactive and impulse turbines. Impulse turbine increases velocity in the nozzle which causes losses hence less efficient compared to reaction turbine. Reaction turbines have a pressure difference at the rotor inlet and exit which leads to tip clearance losses (Zaniewski et al., 2019). Turbine designers have increased the performance of multistage axial flow turbines by making the first 50% stages impulse in design so as to maximize pressure drop and the remaining 50% stages are reactive in design (Gorla & Khan, 2003).

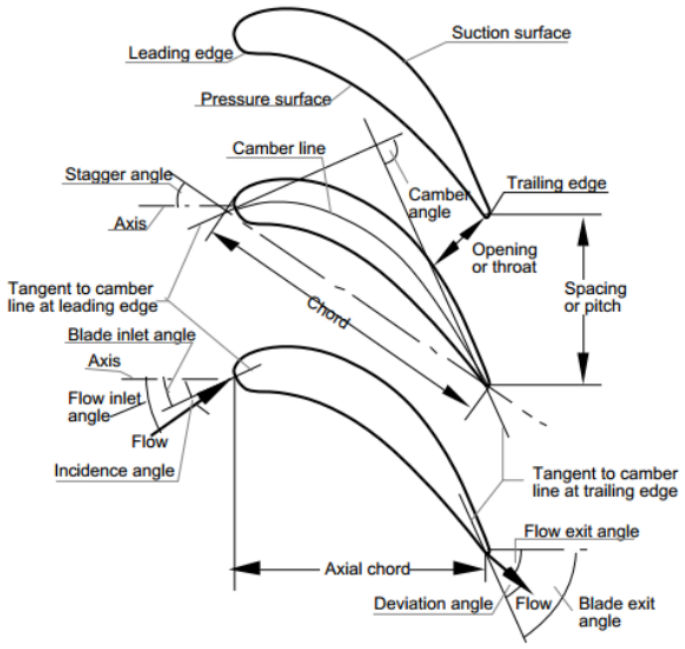

Figure 2.2: Blades of an axial flow turbine stage (Guédez, 2011)

2.4 Variables Affecting Performance of Turbines

The gas turbines performance can be measured by efficiency, power output and torque. Thermal efficiency and power output of gas turbines can be increased by increasing the turbine inlet temperature (TIT) at a fixed pressure. Blade cooling has been used to ensure that the turbine operates at temperatures above the melting point of the blade material(Dongre, Vikas, & Vishal, 2014). Cooling also increases the life cycle of the turbine by reducing the effect of blade thermal stresses(J.-C. Han, 2004). The overall efficiency of a gas turbine increases with increase in pressure ratio at a given temperature(Boyce, 2002). This section explores the key variables and their effect on performance of gas turbines.

2.4.1 Turbine Inlet Temperature

Thermal efficiency of gas turbines can be increased by increasing the turbine inlet temperature (TIT) at a fixed pressure. The current TIT for aircraft is about 1473 to 1773 K and the power can be doubled by increasing the TIT from 1773 to 2273 K (Sunden & Xie, 2010). The turbine blades should be made with a material that can withstand the high inlet temperature (Estrada, 2007). Cooling techniques are also used to ensure the gas turbines operates at temperatures higher than the melting point of blade material (Dongre et al., 2014).

Aminov *et al.* (Aminov, Moskalenko, & Kozhevnikov, 2018) studied the optimal gas turbine inlet temperature (TIT) for cyclic operation using numerical simulation method. The findings were that increase in TIT resulted in increased thermal efficiency, reduced fuel consumption, high thermal and mechanical stresses hence reduced turbine life. The total operation costs of gas turbines increased due to cooling, thermal barriers coating and uneven electrical loads. Gas turbines with lower TIT were more profitable for peak operations with high number of startups and shutdowns. Though gas turbines with higher TIT were more suitable for base load operations due to high fuel efficiency, the effects of TIT on partial load operations were not considered.

Nayak *et al.* (Nayak & Mahto, 2014) studied the effects of gas turbine inlet temperature on combined cycle performance. Thermodynamic model of a simple combined cycle was developed, analyzed and MATLAB software used to simulate the operating conditions. They found that the specific fuel consumption decreased with increase in gas turbine inlet temperature (GTIT). Thermal efficiency and specific work increased with increase in GTIT. The rate of increase in thermal efficiency was slow at higher GTIT due to heat loss. The highest TIT for maximum thermal efficiency was not evaluated.

2.4.2 Blade Cooling

Cooling is used to enable the turbine to operate at temperatures above the melting point of the blade material and prevents wear due to thermal loads(Zhang, Zhu, Xie, Li, & Sunden, 2021). First gas turbine blade cooling was at Conway in 1962 and continues being improved (Xu, Bo, Hongde, & Lei, 2015). The most commonly used techniques are film, convection, impingement and combined cooling. Figure 2.3 shows some internal and external blade cooling techniques. The blade leading edge is cooled by jet impingement with film cooling while the pin-fins with ejection is used to cool trailing edge and the middle part of blade is cooled by internal serpentine ribbed-turbulators passages (Sunden & Xie, 2010). In internal cooling method cold air is tapped from the compressor and directed to the channels of turbine blade (Dongre et al., 2014). Internal cooling provides cools turbine better than other techniques hence increasing the blade life (Nandakumar & Moorthi, 2015).

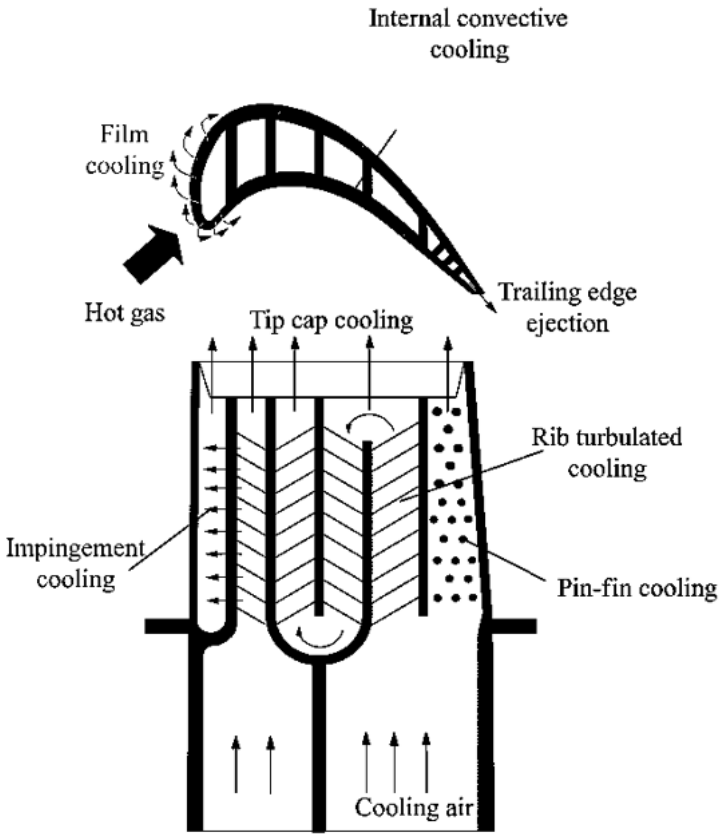

Figure 2.3: Blade cooling techniques (Sunden & Xie, 2010)

Narzary *et al.* (Narzary, Liu, Rallabandi, & Han, 2010) studied the influence of coolant density on turbine blade film-cooling using pressure sensitive paint technique. Pressure sensitive paint technique involves a paint-like coating which fluoresces under a specific illumination wavelength in differing intensities depending on the external air pressure being applied locally to its surface. The results showed that film cooling effectiveness increased with increase in blowing ratio. Film cooling effectiveness increased proportionately to density ratio. Increase in free stream turbulence intensity decreased the film cooling effectiveness. The study showed that turbulence affects film cooling effectiveness, however ways of improving it in turbulent gas flow were not explored.

Sanjay *et al.* (Kumar & Singh, 2014) studied enhancement of combined cycle performance using transpiration cooling of gas turbine blades with steam. Thermodynamic modeling was used to develop a C++ computer code to compare the performance of combined cycle with air and steam cooling. The findings indicated that the combined cycle efficiency and specific work output varied with turbine inlet temperature (TIT) and coolant. As the TIT increased from 1600 K to 1800 K the difference in cycle efficiency between steam and air cooled turbine varied from 1.47% to 2%. The specific work output for a steam cooled combined cycle was 63 kJ/kg higher than air cooled combined cycle at TIT of 1800 K. Although the study established that steam had better cooling characteristics than air, it did not consider the impact of steam generation on overall plant efficiency.

2.4.3 Blade Tip Clearance

Blade tip clearance is the space between the blade and the casing and is responsible for leakage mass flow across the blade tip from the pressure side to the suction side. Tip leakage loss causes a third of all the aerodynamic losses experienced in turbines (Shirzadi & Saeidi, 2012). The leakage results in increased operation cost, reduced engine life and low turbine efficiency due to decreased net work output of each rotor (Qi & Zhou, 2014).

The gas turbine rotation causes blade tip losses due to the vortices formed as the fluid passes between the blades and the casing. Gao *et al.* (J. Gao, Zheng, Liu, & Dong, 2016) studied the effects of blade rotation on axial turbine tip leakage vortex breakdown and loss using numerical method. The findings were that the tip mixing loss per unit leakage flow reduced with increase in rotation speed. The vortex breakdown was influenced by Coriolis force and the 3D shear flow in the casing endwall region. Although the study showed that increased speed reduced the tip mixing loss per unit leakage flow, the rotational speed for optimum reduction in tip leakage flow was not evaluated.

(Shirzadi & Saeidi, 2012) studied the effects of tip clearance on performance of a heavy duty multi stage axial turbine using 3D ANSYS CFX-12 CFD simulation code. It was found that the tip clearance losses of 1^{st} and 2^{nd} rotors were higher than that of the 3^{rd} and 4^{th} rotors. The leakage mass flow of rear rotors was less than that of front ones yet it affected overall efficiency of the turbine significantly. The study showed that leakage mass flow affected turbine's the efficiency. However the influence of cooling fluid on mass flow was not considered.

2.5 Syngas Generation and Utilization in Gas Turbine

2.5.1 Syngas Generation

Gasification is converting fuels such as coal, petroleum coke, biomass, municipal waste and other carbonaceous materials into cleaner and high-value synthesis gas (syngas). Coal gasification is the process of reacting coal with oxygen, steam, and carbon dioxide to form a product gas containing hydrogen, carbon monoxide, carbon dioxide, steam and nitrogen oxide. Syngas is later cleaned to remove the non combustible gases that comprise steam, carbon dioxide and nitrogen oxides (Oluyede & Phillips, 2006). The simplified important reactions are (Agrawal, 2000):

Partial oxidation:

$$C + 1/2O_2 \longrightarrow CO \tag{2.1}$$

Water gas shift:

$$CO + H_2O \longleftrightarrow CO_2 + H_2 \tag{2.2}$$

Methanation:

$$CO + 3H_2 \longleftrightarrow CH_4 + H_2O \tag{2.3}$$

Steam-carbon reaction:

$$C + H_2O \longrightarrow CO + H_2 \tag{2.4}$$

Boudouard reaction:

$$C + CO_2 \longrightarrow 2CO \tag{2.5}$$

Coal gasification is preferred to combustion due to the low emissions per unit of energy produced. Generation of syngas from coal is classified as surface and underground coal gasification depending on location. Underground coal that is not economical to mine is gasified in the mines and the syngas pumped to the surface. In surface coal gasification, coal is mined and reacted on the surface. Syngas is used as fuel gas in gas turbines, as feedstocks for liquid fuels and chemicals (Daggupati et al., 2011).

2.5.2 Syngas Utilization in Gas Turbines

Syngas is a cleaner, low heating value energy source and studies are underway to establish its performance in various applications including power generation (Roach & Ponton, 2013). It is difficult to control the quality of the syngas in cases where the coal has high ash and moisture content, hence reducing the life of turbine components (Bhatt, 2012).

Most of the existing gas turbines are manufactured specifically to burn standard fuels like natural gas and light diesel fuel (Xuelei et al., 2010). Syngas from coal has a low heating value of 16 MJ/kg while natural gas has a heating value of 50 MJ/kg (Johnson, 1991). When using syngas to run a natural gas turbine, the turbine is assumed to operate under off design conditions. This implies that higher syngas flow rate is needed to attain the same firing temperature for the same compressor flow, hence the mass flow rate into the turbine has to be increased (Johnson, 1991). This can only be achieved if Equation 2.6 is satisfied.

$$m_3 = {p_3}^* A_n M / \sqrt{{T_3}^*} \tag{2.6}$$

Where, m_3 is inlet flow of turbine, ${p_3}^*$ is turbine inlet total pressure, ${T_3}^*$ is turbine inlet total temperature, A_n is turbine inlet area, M is constant. Maintaining ${T_3}^*$ as the natural gas temperature. Then total pressure or turbine area must be increased to cater for the high mass flow.

Xuelei *et al.* (Xuelei et al., 2010) studied the influence of firing medium or low heat value fuel on the safe operation of a gas turbine using a calculations model. The safe operating conditions of syngas fired gas turbine such as compressor surge margin, axial torque and turbine metal temperature were evaluated. It was found that increasing the compressor pressure ratio increased the axial torque of the turbine, decreased the compressor surge margin and increased the turbine temperature hence it was not a safe performance strategy. Although it was not safe to increase compression ratio of syngas fired gas turbine, the optimum pressure ratio was not determined in the study.

Oluyede *et al.* (Oluyede & Phillips, 2007) studied the impact of firing syngas in a gas turbine modeled using a GateCycle software. The software was used to predict design and off-design performance of combined and advanced gas turbine cycles. Therefore, in order to attain the firing temperature and maintain constant energy input to the gas turbine a large fuel flow rate was necessary. The high hydrogen content in the syngas resulted to high flame temperature and high moisture content hence affecting the hot section of the material and reducing the life of the turbine. The impact of back pressure as a result of increased mass flow rate was however not investigated.

Chyu *et al.* (Chyu, Siw, Karaivanov, Slaughter, & Alvin, 2009) studied the effects of internal heat transfer of syngas, hydrogen and oxyfuel turbines using FLUENT

flow simulation software. Oxyfuel is produced when syngas is burned with a nearly pure oxygen producing a highly enriched CO_2 gas, steam and excess oxygen. It was found that the leading and trailing edge of hydrogen fired turbine airfoil had hot spots and the metal temperature reduction was through thermal barrier coating (TCB) thickening. The oxyfuel turbines gas side temperature of 2030 K was higher than 1720 K of hydrogen fired turbines, and exceeded the materials limit of 1370 K. The current technology level on aerothermal cooling and TBC protection forms a basis for further studies to develop future oxyfuel turbine systems that are viable and durable at high moisture content.

Maurstad (Maurstad, 2005) and Barnes (Barnes, 2013) did a review on existing Coal based Integrated Gasification Combined Cycle (IGCC) Technology. The findings were that to increase efficiency and still reduce emissions would was a challenge. The high moisture content in syngas lead to reduced operating hours of natural gas turbines. Hence studies and experiment to optimize and validate a tradeoffs between efficiency, reliability, availability and maintainability need to be done. Further development of advanced materials to handle high moisture and gas temperature is required.

2.6 Summary of Gaps

The performance of a gas turbine especially when using syngas can be improved. Below are some gaps identified in the literature;

1. The current technology level on aerothermal cooling and thermal barrier coating (TBC) protection forms a basis for further studies to develop future oxyfuel turbine systems that are viable and durable at high moisture content.
2. The studies show that increased rotational speed reduced the tip mixing loss. Further research is required to determine the rotational speed for optimum

reduction in tip leakage.

3. Although it was not safe to increase compression ratio of syngas fired gas turbine, the highest pressure ratio for maximum efficiency was not determined in the study.

4. The studies showed that leakage mass flow affected the efficiency of the turbine, however the influence of cooling fluid on mass flow was not considered.

5. Firing syngas in a natural gas turbine requires increased mass flow rate however the impact of back pressure that results was however not investigated.

6. Research shows that turbulence affects film cooling effectiveness, making it important to explore ways of improving film cooling effectiveness in turbulent gas flow.

CHAPTER THREE

METHODOLOGY

3.1 Background

The problem of energy crisis has led to the demand of cheap, clean and reliable sources. This research involves a study of behaviour of gas expanding in a turbine running on coal syngas from Mui Basin. Performance of an axial flow turbine running on syngas was simulated based on solution of flow governing equations. Therefore this chapter presents the computational domain around the flow region, the flow governing equations and the solution technique used in the performance simulation.

3.2 Modeling of Syngas Turbine

The axial flow turbine rotor model was developed using BladeGen of the ANSYS workbench 17.2 to be used in the syngas simulation. Eighteen blades were selected for the model since they provided good and high efficiency flow for small scale turbine (Ennil & Mahmouda, 2015) and they were even in number for dynamic balance and to minimize potential vibrations (Nagpurwala, 2012). Blade configuration was selected based on a criteria utilized for NASA aerofoil profile for uncooled single stage turbines for high efficiency operation (Gardner, 1979). The rotor model developed was sized to blade height of 25 mm, hub diameter of 60 mm and tip diameter of 110 mm. These dimensions were close to those of available axial micro turbines (Kosowski, Piwowarski, Stepien, & Włodarski, 2012). Figure 3.1 shows the rotor model, while Table 3.1 illustrates the blade features selected following the criteria above.

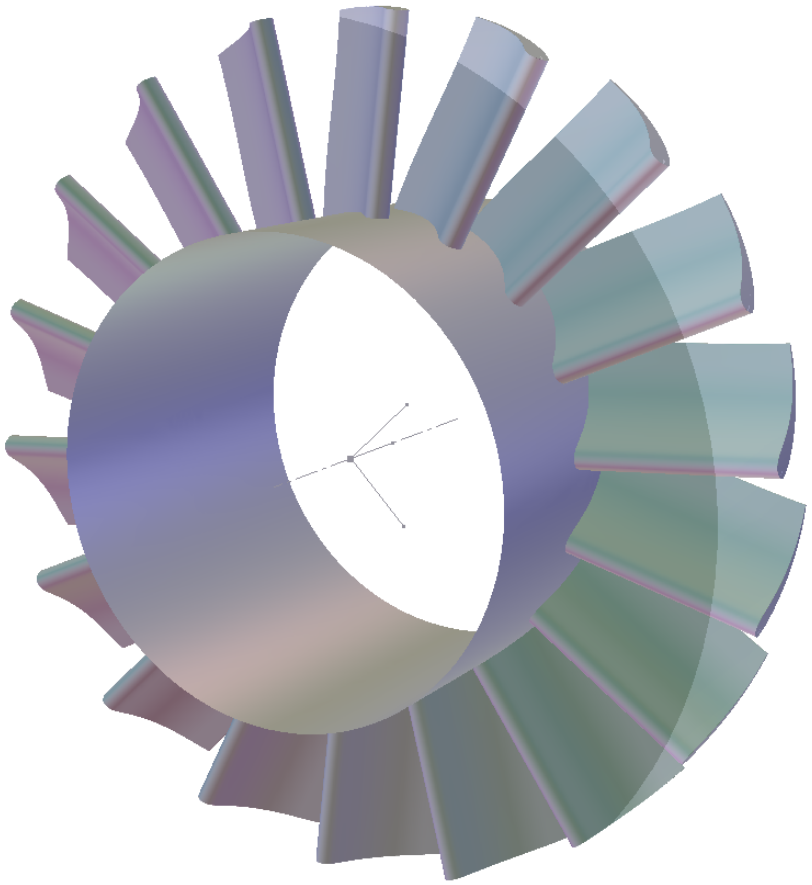

Figure 3.1: Rotor model with 18 blades

Table 3.1: Rotor blade details

Parameter	Value
Number of Blades	18
Inlet Angle β_{in}	40.2
Exit Angle β_{out}	72.4
Blade Height	25 mm
Hub Diameter	60 mm
Tip Diameter	110 mm

3.3 CFD Modeling

The performance of turbine design was modeled using CFD code ANSYS Workbench and CFX 17.2 academic version. The computational domain used was flow across

one blade since it modeled behaviour of fluid in gas turbine rotor. Syngas combustion gases were used as computation fluid in simulation. Finite volume approach which is convenient to use with unstructured grids, was used to discretize the steady flow three dimensional Navier-Stoke equation for compressible flow and the energy equation (Bari, David, Torresi, Fortunato, & Camporeale, 2014). Equation 3.2, 3.3 and 3.4 are the three Navier Stokes equations expressed in the spatial and temporal coordinates x,y,z and t. The conservation equations are (Bari et al., 2014);

(i) Mass conservation equation

$$\frac{\partial u}{\partial x} + \frac{\partial v}{\partial y} + \frac{\partial w}{\partial z} = 0 \tag{3.1}$$

(ii) x momentum conservation equation

$$\frac{\rho Du}{Dt} = -\frac{\partial P}{\partial x} + \mu \left(\frac{\partial^2 u}{\partial x^2} + \frac{\partial^2 u}{\partial y^2} + \frac{\partial^2 u}{\partial z^2} \right) + \rho g_x \tag{3.2}$$

(iii) y momentum conservation equation

$$\frac{\rho Dv}{Dt} = -\frac{\partial P}{\partial y} + \mu \left(\frac{\partial^2 v}{\partial x^2} + \frac{\partial^2 v}{\partial y^2} + \frac{\partial^2 v}{\partial z^2} \right) + \rho g_y \tag{3.3}$$

(iv) z momentum conservation equation

$$\frac{\rho Dw}{Dt} = -\frac{\partial P}{\partial z} + \mu \left(\frac{\partial^2 w}{\partial x^2} + \frac{\partial^2 w}{\partial y^2} + \frac{\partial^2 w}{\partial z^2} \right) + \rho g_z \tag{3.4}$$

(v) Energy equation

$$C_p \frac{D\rho T}{Dt} = \lambda \left(\frac{\partial^2 T}{\partial x^2} + \frac{\partial^2 T}{\partial y^2} + \frac{\partial^2 T}{\partial z^2} \right) - \frac{\partial}{\partial x} \left(\rho T \sum_{i=1}^{N} C_{pi} D_i \frac{\partial Y_i}{\partial x} \right) - \frac{\partial}{\partial y} \left(\rho T \sum_{i=1}^{N} C_{pi} D_i \frac{\partial Y_i}{\partial y} \right) - \frac{\partial}{\partial z} \left(\rho T \sum_{i=1}^{N} C_{pi} D_i \frac{\partial Y_i}{\partial z} \right) - \sum_{i=1}^{N} \omega_i \Delta h^o_{f,i}. \tag{3.5}$$

(vi) Bernoulli's equation

$$P + \frac{1}{2}\rho v^2 + \rho g h = Constant \tag{3.6}$$

(vii) Velocity equation

$$v = \sqrt{\frac{\gamma RT}{M}} \tag{3.7}$$

(viii) Gay-Lussacs law

$$\frac{P}{T} = constant \tag{3.8}$$

(ix) Power equation

$$\begin{aligned} p &= \tau\omega \\ \omega &= 2\pi N_{rpm}/60 \end{aligned} \tag{3.9}$$

Pressure ratio (r_P)

$$r$$

$$_P = \mathrm{P}_{inlet} \overline{P_{outlet}(3.10)}$$

Thermal efficiency

$$\eta_{th} = \left\{ 1 - \frac{T_{TET}}{T_{TIT}} \right\} \times 100 \tag{3.11}$$

Correlation coefficient

$$r = \frac{n\left(\sum ab\right) - \left(\sum a\right)\left(\sum b\right)}{\sqrt{\left[n\sum a^2 - \left(\sum a\right)^2\right]\left[n\sum b^2 - \left(\sum b\right)^2\right]}} \tag{3.12}$$

Where u, v and w are the velocity components (m/s) in the x, y and z directions respectively, ρ is the density (kg/m*3), P is the pressure (bar), g is acceleration due to gravity (N/kg), h is elevation (m), γ is adiabatic constant, R is specific gas constant (kJ/kg.K), M is molecular mass (kg/mol), T is the temperature (K), λ is the thermal conductivity (W/(m·K)), μ is the dynamic viscosity (kg/(m.s)), D is the diffusivity, p is power (W), τ is torque (Nm), ω is the angular velocity (rad/s), π=3.14, P_{inlet} is pressure at inlet (bar), P_{outlet} is pressure at outlet (bar), η_{th} is thermal efficiency T_{TET} is turbine exit temperature (K), T_{TIT} is turbine inlet temperature (K), r is correlation coefficient, n is number in the given dataset, a is first variable in the context and b is second variable.

3.3.1 Mesh Generation and Analysis

The computation domain was developed in ANSYS design modeler and meshing tool. Unstructured grid mesh was selected due to high flexibility level and control of grid cell shape and size (Zikanov, 2010). 3-Dimension tetrahedral grids were chosen to cater for the complex domain around the blade. The computational domain was developed for one blade since the flow behaviour was similar for all blades. Figure 3.2 shows the computational domain before meshing while the meshed domain with exploded view of trailing and leading edges is shown in Figure 3.3.

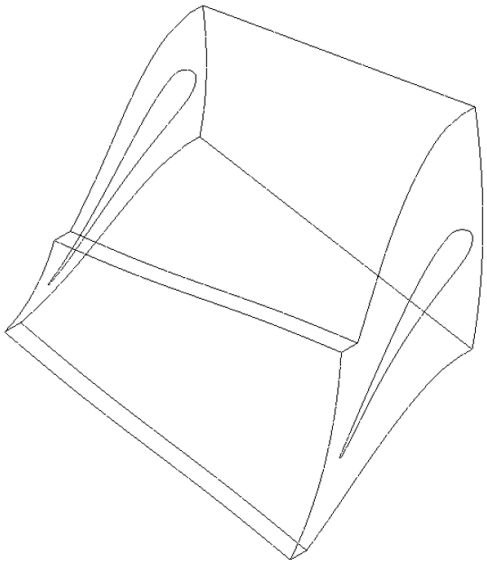

Figure 3.2: Computational domain before meshing

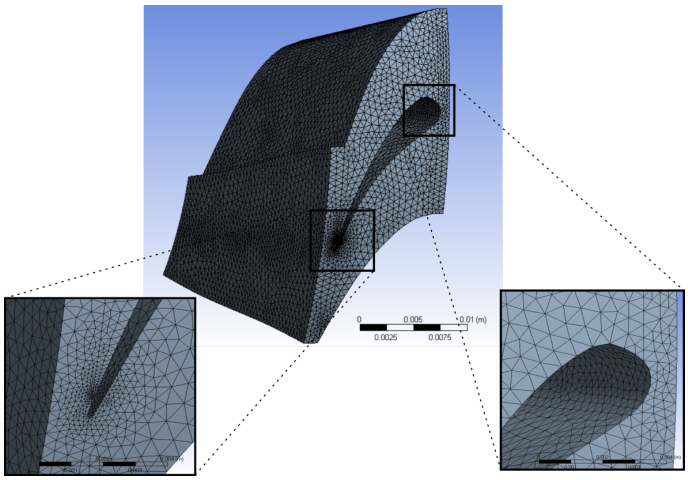

Figure 3.3: Exploded view of the 3D meshed domain

The mesh independence study was carried out to determine accuracy of numerical results and their behaviour with varying cell numbers. Flow simulations were carried out for mesh cells ranging from 212,471 to 5,628,720 and the performance of each case is as shown by Figure 3.4. There was a 0.09% change in efficiency with increase in number of cells above 1,857,744. Therefore to save on simulation resources and due to computer processor limitations, 1,857,744 cells were adopted to study the

flow and temperature distribution of expanding syngas in gas turbine. Computer with Microsoft Windows 10, 64 bits operating system, Intel(R) Core(TM)i7-7700HQ CPU@ 2.80GHz processor, with 16.0 GB RAM installed memory was used for the simulation.

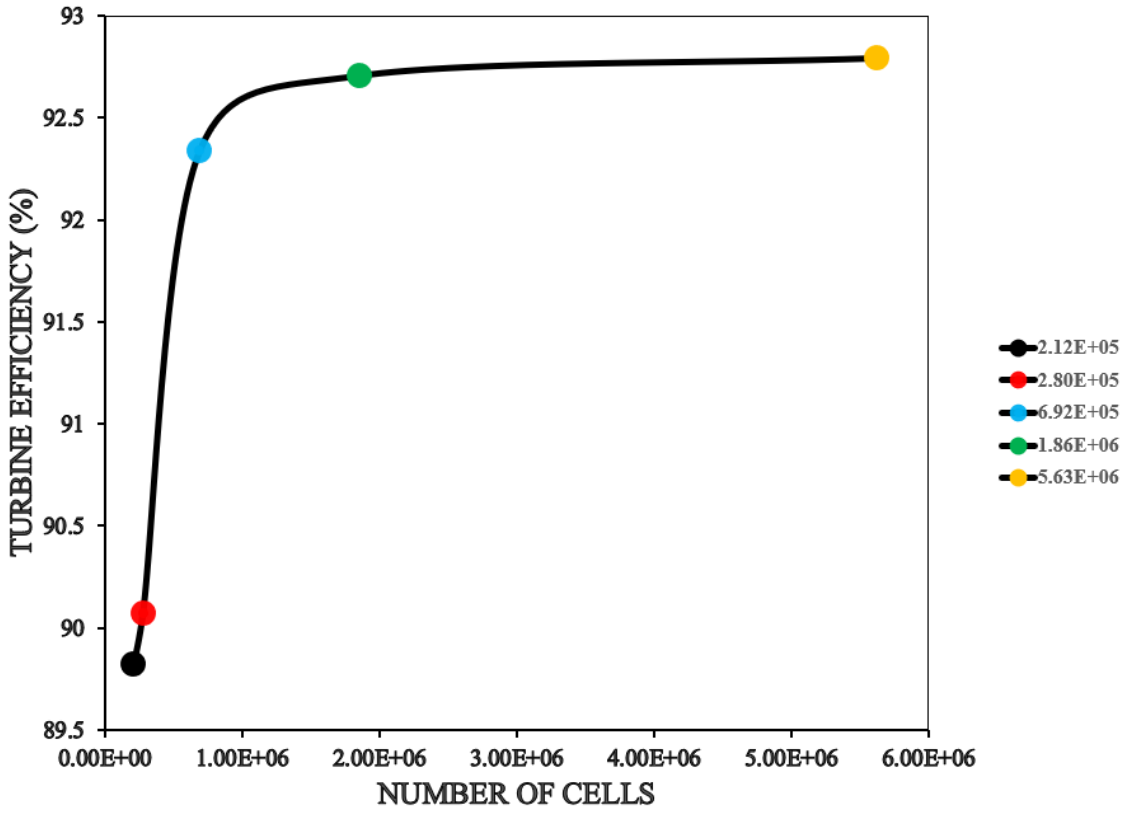

Figure 3.4: Mesh sensitivity analysis

3.3.2 Developed Simulation Model Validation

Shown in Figure 3.5 is the efficiency of rotor at various pressure ratio. Simulation results were obtained using the developed model while experimental ones are from literature (Dubitsky, Weidermann, Nakano, & Perera, 2003). The experimental and simulation curves indicated a correlation coefficient (r) of 0.9454. Correlation coefficient was close to unity meaning that the predicted efficiency data could be used to represent experimental data. This means that the simulation model was

valid and suitable for in further analysis.

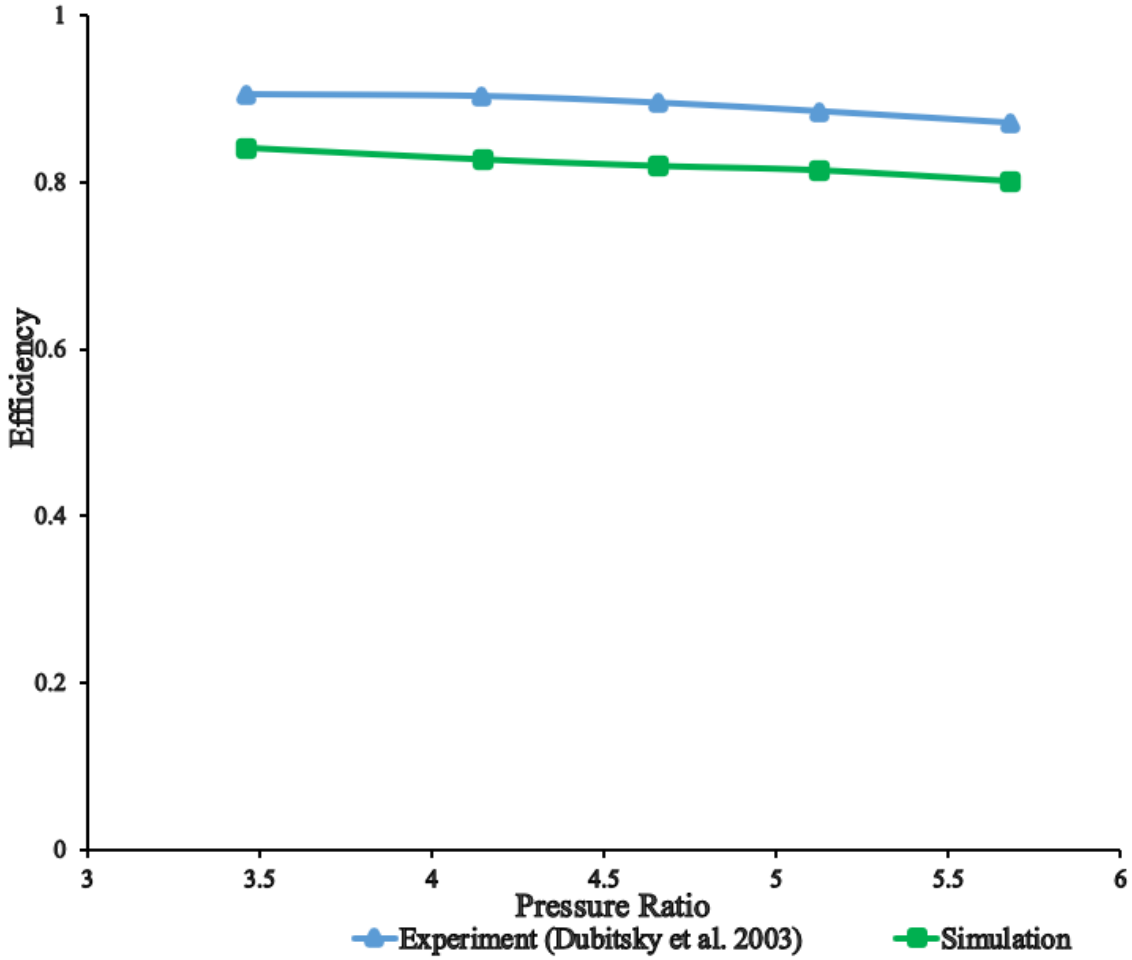

Figure 3.5: Variation of rotor efficiency with pressure ratio

3.3.3 Boundary conditions

Total temperature and total pressure were specified at the inlet while static pressure was set at the outlet. Figure 3.6 shows inlet pressure of 10 bar and temperature of 900 K, outlet pressure of 1 bar, adiabatic, no slip and smooth wall and flow direction. The exit pressure was fixed at 1 bar, while the inlet pressure and temperature were specified for different simulations.

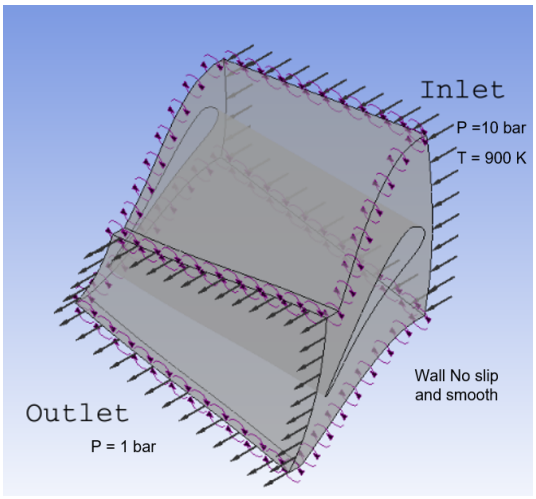

Figure 3.6: Flow path, inlet and outlet

In the present research the rotational speed, turbine inlet temperature (TIT) and pressure ratio were each varied while keeping the other variables constant to study their effect on gas turbine performance. The turbine inlet temperature and pressure ratio were assumed to be 900 K and 10 respectively, while the rotational speed was varied in steps of 1000 rpm. The lower limit of 3000 rpm was based on design limit guided by the first power generating turbine while the upper limit of 14000 rpm was based on a split shaft gas turbine design (Lazzaretto & Toffolo, 2001), (ASME, 2007), (Roberts & Kubasco, 1982). In addition a pressure ratio of 10 was selected as it coincides with that of micro turbines (Kosowski et al., 2012). The TIT of 900 K was below temperature of uncooled blade (973 K) and higher than the lower temperature coolant (800 K). The coolant air is bled from compressor exit and since the compressed air is mixed with fuel and combusted the turbine must operate at a higher temperature than the compressor (Bhargava et al., 2007), (Mazzotta, Chyu, & Alvin, 2007).

Pressure ratio and rotational speed were assumed to be 10 and 10,000 rpm respectively, while turbine inlet temperature (TIT) was varied in steps of 100 K from 600 K to 1800 K. Turbine inlet temperature of 1800 K is for a steam cooled

blade above which thermal coating of the blades is required(Xu et al., 2015) while 600 K is almost equal to TIT of the first simple gas turbine designed in 1903 (Bhargava et al., 2007). The pressure ratio was varied from 5 to 20 in steps of 5, while turbine inlet temperature and rotational speed were maintained at 900 K and 10000 rpm, respectively. The pressure ratios of 5 and 20 were close to those of the first simple gas turbine designed in 1903 and in the range of syngas turbine respectively (Bhargava et al., 2007), (Kim, Lee, Kim, Sohn, & Joo, 2010). Table 3.2 shows the boundary conditions used in simulation for the research.

Table 3.2: Boundary conditions

Variable	Limits
Reference Pressure	1 Bar
Rotational Speed	3000 rpm to 14000 rpm
Turbine Inlet Temperature	600 K to 1800 K
Pressure Ratio	5 to 20
Out flow Static pressure	1 Bar
Fluid	Syngas (Combustion products)
	Natural gas (Combustion products)
	Ideal gas (Air)

3.3.4 Syngas Combustion Equations

The composition of coal in Kenya ranges from lignite to sub-bituminous. The main components of syngas from lignite coal are hydrogen gas (H_2) at 28.5% and carbon monoxide gas (CO) at 39.7% (Kariuki & Kuria, 2021), (Wang & Gary, 2017) (Ghenai, 2010). The stoichiometric combustion equations of hydrogen and carbon monoxide gases expressed as follows;

1. Hydrogen combustion

$$2H_2 + O_2 \rightarrow 2H_2O \tag{3.13}$$

Multiplying through by 0.285

$$0.285 \times 2H_2 + 0.285 \times O_2 \rightarrow 2 \times 0.285H_2O \tag{3.14}$$

$$0.57H_2 + 0.285O_2 \rightarrow 0.57H_2O \tag{3.15}$$

2. Carbon monoxide combustion

$$2CO + O_2 \rightarrow 2CO_2 \tag{3.16}$$

Multiplying through by 0.397

$$0.397 \times 2CO + 0.397 \times O_2 \rightarrow 2 \times 0.397CO_2 \tag{3.17}$$

$$0.794CO + 0.397O_2 \rightarrow 0.794CO_2 \tag{3.18}$$

Natural gas consist mainly of methane at 95.7%, the stoichiometric combustion equations expressed as follows;

$$CH_4 + 2O_2 \rightarrow CO_2 + 2H_2O \tag{3.19}$$

Multiplying through by 0.95

$$0.95 \times CH_4 + 0.95 \times 2O_2 \rightarrow 0.95 \times CO_2 + 2 \times 0.95 \times H_2O \tag{3.20}$$

$$0.95CH_4 + 1.9O_2 \rightarrow 0.95CO_2 + 1.9H_2O \tag{3.21}$$

The flow around the blade was simulated using syngas combustion and natural gas combustion to compare the performance. The syngas combustion was assumed to consist of products of stoichiometric combustion of hydrogen as shown in Equation 3.15 and carbon monoxide as shown in Equation 3.18 from lignite coal which is similar to coal available in Kenya (Kariuki & Kuria, 2021),(Wang & Gary, 2017). The syngas combustion gases fluid material was not available in the Ansys CFX and it was created consisting of ideal CO_2

and H_2O gases at mass fractions of 0.5821 and 0.4179 respectively. Similarly the natural gas fluid material combustion gases were formed were at a ratio of 0.3333 CO_2 and 0.6667 H_2O as shown by Equation 3.21 (Ganjikunta P.E, 2015). The water and carbon dioxide were a fraction to form a fluid with two components.

3.3.5 Turbulence Modeling of Flow Equations

Turbulence is flow disturbance and boundary layer separation caused by change in pressure and velocity. The type of flow in a gas turbine can be determined by the dimensionless Reynolds number (Re) shown by Equation 3.22. Where ρ is fluid density (kg/m^3), U is flow velocity (m/s), L is length scale (m) and μ is dynamic viscosity (kg/m s). The flow is laminar at Re < 2300, transient at $2300 <$ Re < 4000 and turbulent at Re > 4000. The flow of syngas combustion gases in the computational domain was turbulent with a Reynolds number of 2.2 $\times 10^5$ calculated by substituting the values in Equation 3.22 as (U) is flow velocity at rotational speed of 10,000 rpm = 61.8611 m/s, (ρ) is syngas density = 4.0262 kg/m^3, (L) is reference radius of the rotor = 0.05 m and (μ) is syngas dynamic viscosity = 5.61 $\times 10^{-5}$ kg/m s.

$$Re = \frac{\rho.U.L}{\mu}, \tag{3.22}$$

Reynolds-Averaging is the first step in modeling of turbulent flow equations. The flow equations were averaged in order to deal with the effect of fluctuating components of the turbulent flow as shown in Equation 3.23 (Zikanov, 2010).

$$\rho \frac{\partial}{\partial x_j}\left(\overline{u}_i \overline{u}_j\right) - = \frac{\partial P}{\partial x_i} + \frac{\partial}{\partial x_j}\left(\mu\left[\frac{\partial \overline{u}_i}{\partial x_j} + \frac{\partial \overline{u}_j}{\partial x_i}\right] - \rho\overline{\acute{u}_i \acute{u}_j}\right), \frac{\partial \overline{u}_i}{\partial x_i} = 0 \tag{3.23}$$

Where $\overline{u}_i$, $\overline{u}_j$ are the mean values, $\acute{u}_i$, $\acute{u}_j$ are the fluctuating components and

$-\rho\overline{\acute{u}_i\acute{u}_j}$ are the Reynolds stresses. The Reynolds Stresses were calculated using eddy viscosity turbulence models as

$$-\rho\overline{\acute{u}_i\acute{u}_j} = \mu_t\left(\frac{\partial\overline{u}_i}{\partial x_j} + \frac{\partial\overline{u}_j}{\partial x_i}\right) - \frac{2}{3}\rho k\delta_{ij} \tag{3.24}$$

$$\mu_t = \frac{\rho k}{\omega} \tag{3.25}$$

Where δ_{ij} is the Kronecker second-order tensor. $\delta_{ij} = 1$ if i = j, and $\delta_{ij} = 0$ if i $\neq$ j.

The turbulent models available in CFD are; the Spalart-Allmaras model, the Reynolds Stress Model, the k-$\epsilon\hat{I}$ model, the k-ω model and the k-ω SST model(Chang & Tavoularis, 2009). k-$\epsilon\hat{I}$ is used in the wake region of the boundary layer away from surface due to it's poor performance in flows with separation(Menter, 1994). k-ω is preferred to k-$\epsilon\hat{I}$ in predicting adverse pressure gradient boundary layer incompressible flows(Soghe, Innocenti, Andreini, & Poncet, 2010). In this work shear-stress transport (SST) ω model was used as it combines both k-ω and k-$\epsilon\hat{I}$ models to accurately predict the flow in aerodynamic applications(Menter, 1994). In the flow simulation k-$\epsilon\hat{I}$ was used in the free stream regions from the inlet to leading edge and from trailing edge to the outlet. The k-ω was used from leading edge to the trailing edge to clearly show pressure gradient and shear stress distributions near and on the blade surface. The SST ω model as shown in Equation 3.26, 3.27 and constants used are shown in Equation 3.32.

$$\frac{D\rho k}{Dt} = \tau_{ij}\frac{\partial u_i}{\partial x_j} - \beta^*\rho\omega k + \frac{\partial}{\partial x_j}\left[\left(\mu + \sigma_k\frac{\rho k}{\omega}\right)\frac{\partial k}{\partial x_j}\right] \tag{3.26}$$

$$\begin{aligned}\frac{D\rho\omega}{Dt} =& \frac{\alpha\omega}{k}\tau_{ij}\frac{\partial u_i}{\partial x_j} - \beta\rho\omega^2 + \frac{\partial}{\partial x_j}\left[\left(\mu + \sigma_\omega\frac{\rho k}{\omega}\right)\frac{\partial\omega}{\partial x_j}\right] + \\ & 2\left(1 - F_1\right)\frac{\partial\rho\sigma_{\omega 2}}{\partial\omega}\frac{\partial k}{\partial x_j}\frac{\partial\omega}{\partial x_j}\end{aligned} \tag{3.27}$$

Where,

$$\tau_{ij} = \frac{\rho k}{\omega}\left\{\frac{\partial u_i}{\partial x_j} + \frac{\partial u_j}{\partial x_i} - \frac{2}{3}\frac{\partial u_k}{\partial x_k}\delta_{ij}\right\} - \frac{2}{3}\rho k\delta_{ij} \tag{3.28}$$

$$F_1 = tanh(arg_1^4) \tag{3.29}$$

$$arg_1 = min\left[max\left(\frac{\sqrt{k}}{\beta^*\omega d}, \frac{500v}{d^2\omega}\right), \frac{4\rho\sigma_{\omega 2}}{CD_{k\omega}d2}\right] \tag{3.30}$$

$$CD_{k\omega} = max\left(2\rho\sigma_{\omega 2}\frac{1}{\omega}\frac{\partial k}{\partial x_j}\frac{\partial\omega}{\partial x_j}, 10^{-20}\right) \tag{3.31}$$

$$\sigma_k = 0.85, \sigma_{\omega 1} = 0.5, \beta^* = 0.09, \beta = \frac{3}{40}, \alpha = \frac{5}{9}, \tag{3.32}$$

CHAPTER FOUR

RESULTS AND DISCUSSION

4.1 Background

This chapter presents the results and discussions of performance of syngas and natural gas combustion gases expansion in gas turbines rotor model with varying parameters (rotational speed, pressure ratio and turbine inlet temperature). The sustainable utilization of coal, as noted in this study, is through conversion to syngas. It is important to study the behaviour of syngas combustion gases as they expand across a gas turbine. Therefore, this chapter presents a numerical analysis of flow, temperature, and pressure fields as well as the turbine efficiency that impact on power output.

4.2 Convergence Analysis

CFD governing equations are nonlinear and have no exact solution, hence iterative process was used to achieve a stable and consistent solution for convergence to occur. The residuals of mass, momentum, energy and turbulence equations were monitored to determine the convergence of the simulation. Root Mean Square (RMS) convergence criteria was used with a default criterion of 1e-04.

4.2.1 Syngas Combustion Gases Solutions Convergence

The mass and momentum solutions converged as shown in Figure 4.1. RMS P-Mass is the root mean square residual of mass conservation equation, RMS U-Mom is root mean square residual of momentum conservation of velocity in the X direction, RMS V-Mom is root mean square residual for momentum conservation of velocity in the Y direction and RMS W-Mom is root mean

square residual for momentum conservation of velocity in the Z direction. The calculation solutions converged after 800 iterations at a convergence criterion of between 1.0e-5 and 1.0e-08.

The energy solutions converged as shown in Figure 4.2. RMS H-Energy is the root mean square residual of energy equation. The calculation solutions converged after 100 iterations at a convergence criterion of between 1.0e-5 and 1.0e-6.

The turbulence solutions converged as shown in Figure 4.3. RMS K-TurbKE is the root mean square residual of turbulence kinetic energy. RMS O-TurbFreq is the root mean square residual of turbulence frequency. The calculation solutions converged after 1000 iterations at a convergence criterion of between 1.0e-6 and 1.0e-7.

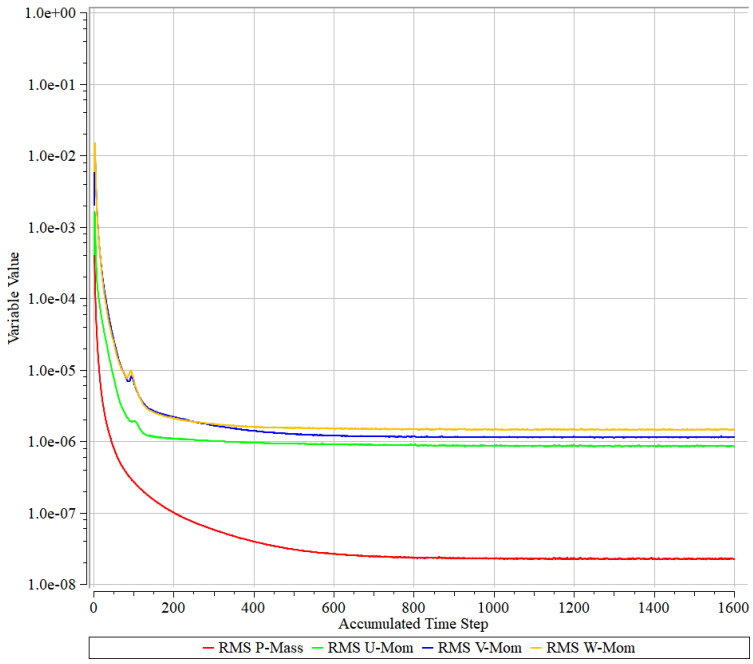

Figure 4.1: Syngas mass and moment conservation convergence

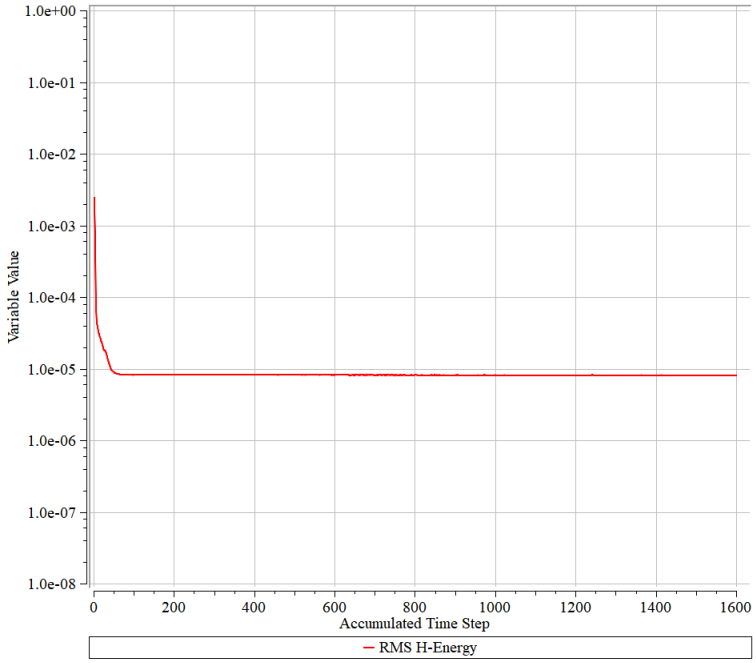

Figure 4.2: Syngas heat transfer convergence

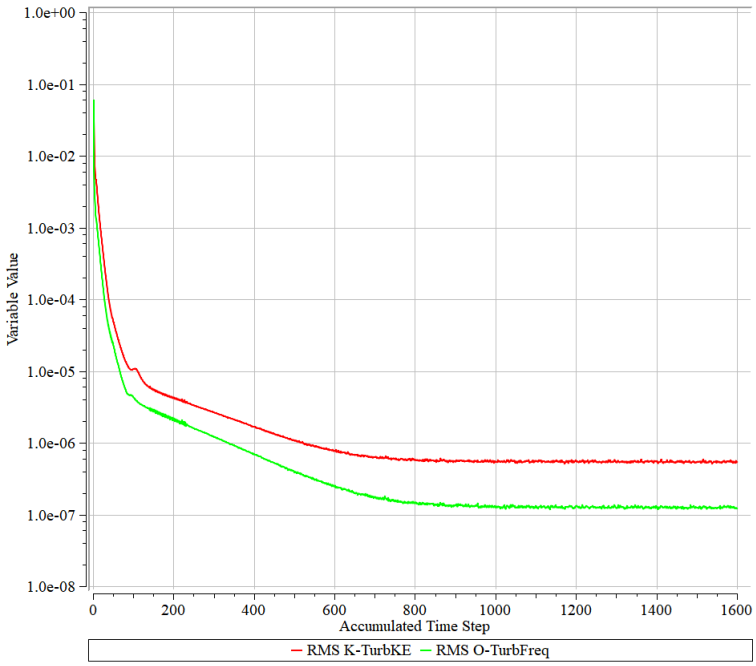

Figure 4.3: Syngas turbulence convergence

4.2.2 Natural Gas Combustion Gases Solutions Convergence

The mass and momentum solutions converged as shown in Figure 4.4. RMS P-Mass is the root mean square residual of mass conservation equation, RMS U-Mom is root mean square residual of momentum conservation of velocity in the X direction, RMS V-Mom is root mean square residual for momentum conservation of velocity in the Y direction and RMS W-Mom is root mean square residual for momentum conservation of velocity in the Z direction. The calculation solutions converged after 600 iterations at a convergence criterion of between 1.0e-5 and 1.0e-08.

The energy solutions converged as shown in Figure 4.5. RMS H-Energy is the root mean square residual of energy equation. The calculation solutions converged after 100 iterations at a convergence criterion of between 1.0e-5 and 1.0e-6.

The turbulence solutions converged as shown in Figure 4.6. RMS K-TurbKE is the root mean square residual of turbulence kinetic energy. RMS O-TurbFreq is the root mean square residual of turbulence frequency. The calculation solutions converged after 1200 iterations at a convergence criterion of between 1.0e-6 and 1.0e-7.

4.2.3 Air Solutions Convergence

The mass and momentum solutions converged as shown in Figure 4.7. RMS P-Mass is the root mean square residual of mass conservation equation, RMS U-Mom is root mean square residual of momentum conservation of velocity in the X direction, RMS V-Mom is root mean square residual for momentum conservation of velocity in the Y direction and RMS W-Mom is root mean square residual for momentum conservation of velocity in the Z direction. The calculation solutions converged after 800 iterations at a convergence criterion

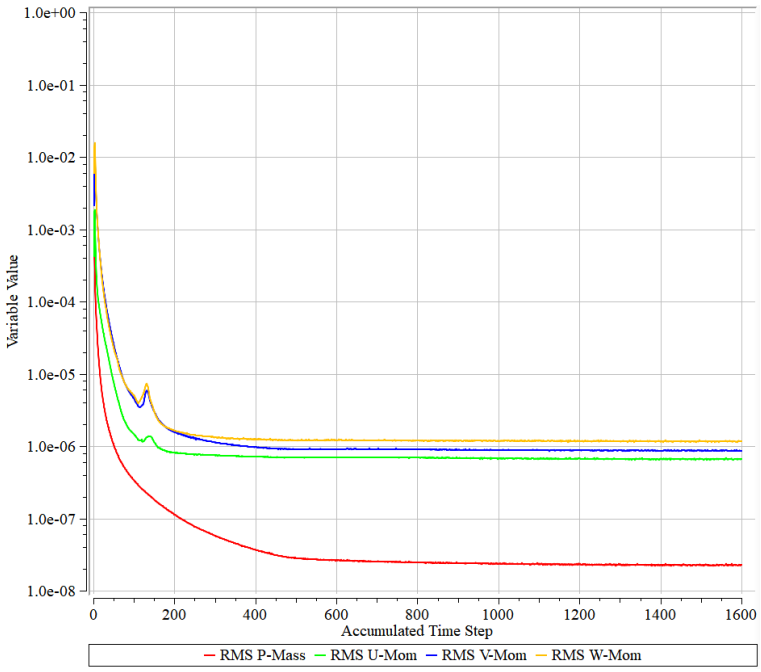

Figure 4.4: Natural gas mass and moment conservation convergence

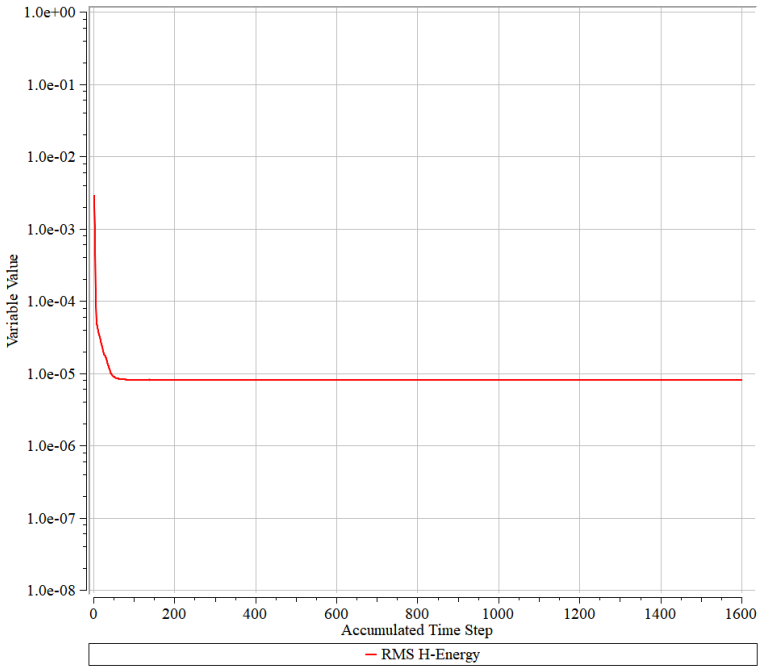

Figure 4.5: Natural gas heat transfer convergence

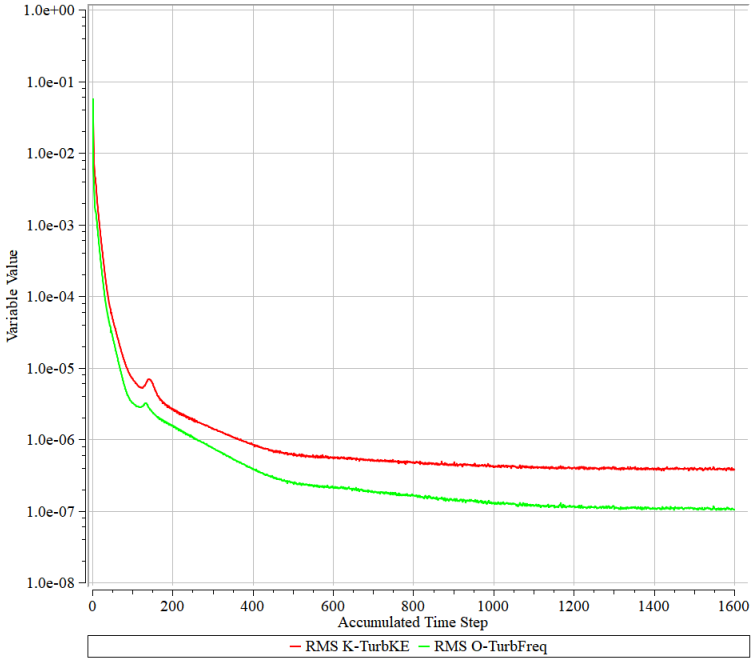

Figure 4.6: Natural gas turbulence convergence

of between 1.0e-05 and 1.0e-8.

The energy solutions converged as shown in Figure 4.8. RMS H-Energy is the root mean square residual of energy equation. The calculation solutions converged after 100 iterations at a convergence criterion of between 1.0e-05 and 1.0e-6.

The turbulence solutions converged as shown in Figure 4.9. RMS K-TurbKE is the root mean square residual of turbulence kinetic energy. RMS O-TurbFreq is the root mean square residual of turbulence frequency. The calculation solutions converged after 1000 iterations at a convergence criterion of between 1.0e-6 and 1.0e-7.

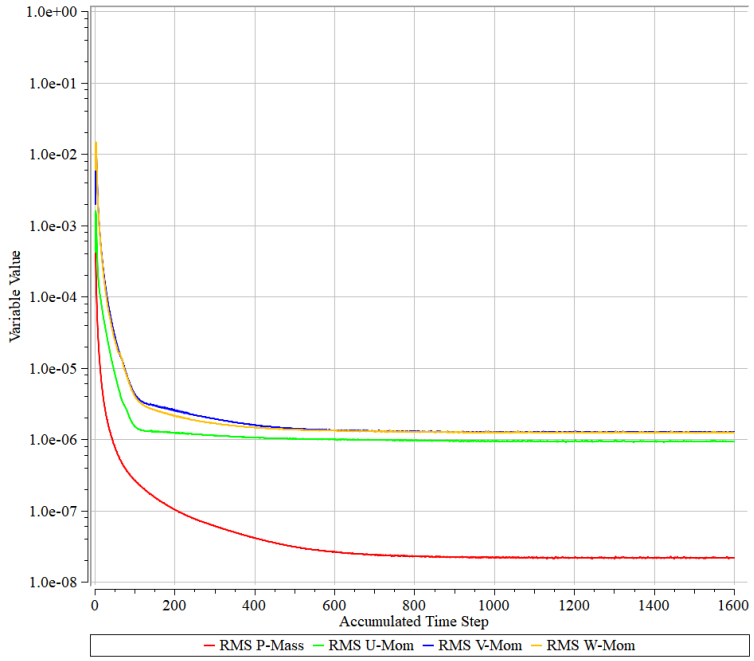

Figure 4.7: Air mass and moment conservation convergence

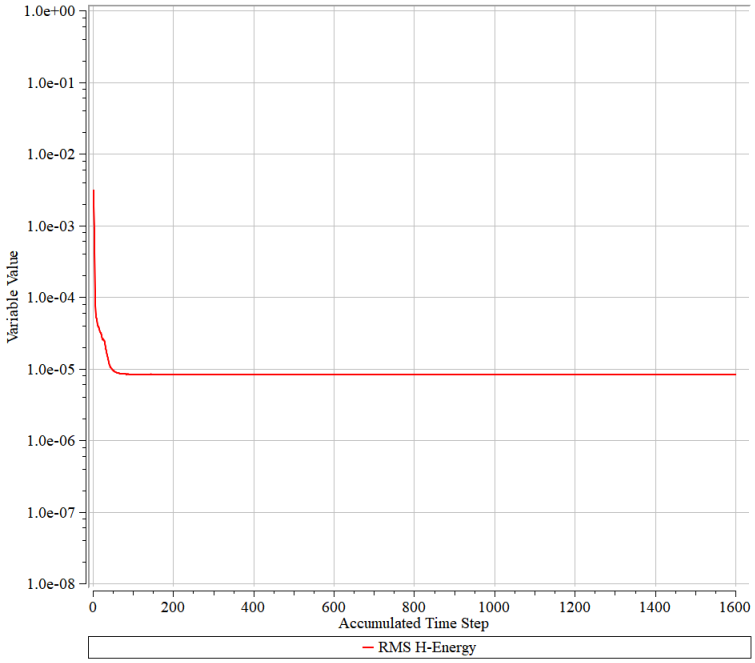

Figure 4.8: Air heat transfer convergence

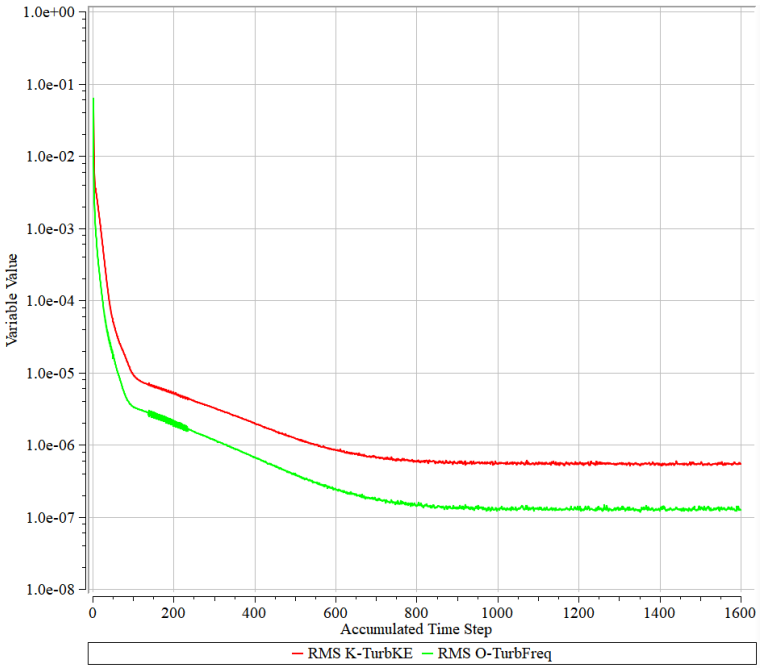

Figure 4.9: Air turbulence convergence

4.3 Flow Field Behavior

The flow field behaviour was be demonstrated by the pressure and velocity distribution as combustion gases expanded across the turbine. The areas with significant change in flow behaviour are pressure side, suction side, leading edge and trailing edge of the turbine blade as shown in Figure 4.10 (a) in which the pressure side is noted to be concave in shape. Figure 4.10 (b) shows the inlet, outlet and the flow direction in the computational domain should also be clear when dealing with flow field.

Figure 4.11 shows pressure distribution from the inlet to the outlet of the flow path representing the computational domain at rotational speeds of ,000 rpm, 6,000 rpm, 9,000 rpm and 12,000 rpm respectively. The upper rotational speed of 12000 rpm was used since there was a significant change in pressure observed at that point. The pressure decreased from inlet to outlet as a result of increase in flow velocity (Darshan, Annigeri, & Kumar, 2016). The pressure was highest

at the tip of the leading edge possibly due to flow separation as the fluid strikes the blade. As the flow speed increased from 3,000 rpm to 12,000 rpm the high pressure region at the leading edge also increased by 1%. The high pressure was due to increased flow separation caused by increase in fluid speed. Figure 4.11 (c) and (d) shows development of a low pressure region on the pressure side of the blade's leading edge. The low pressure region developed due to a separation bubble caused by the increased fluid speed (Acharya & Mahmood, 2006). The pressure difference between the inlet and outlet can be attributed to gas expansion in the turbine to generate energy (Soares, 2015). The high pressure region in the blade trailing edge is due to gas recirculation caused by increased rotational speed.

Shown in Figure 4.12 is pressure distribution from the inlet to the outlet of the flow path representing the computational domain at turbine inlet temperature of 600 K, 1,000 K 1,400 K and 1,800 K, respectively. The pressure at mid point of pressure side decreased by 1% as the turbine inlet temperature increased from 600 K to 1,800 K. The pressure region at the leading edge also decreased. The decrease in pressure could be attributed to increase in kinetic energy due to increase in temperature of the flowing fluid.

Shown in Figure 4.13 is velocity contours across the turbine flow path at rotational speed of 3,000 rpm, 6,000 rpm, 9,000 rpm and 12,000 rpm respectively. The velocity on the suction side of the blade increased from the inlet to the outlet. The high velocity region on the suction side shifted from the leading edge to 0.25 of blade span. That can be attributed to separation line attachment point moving with increase in fluid speed.

Shown in Figure 4.14 is velocity contours across the turbine flow path at pressure ratios of 5, 10, 15 and 20 respectively. The velocity on the suction side of the blade increased from the inlet to the outlet. The velocity at mid point of the suction side of the blade decreased by 75% with increase in pressure ratio

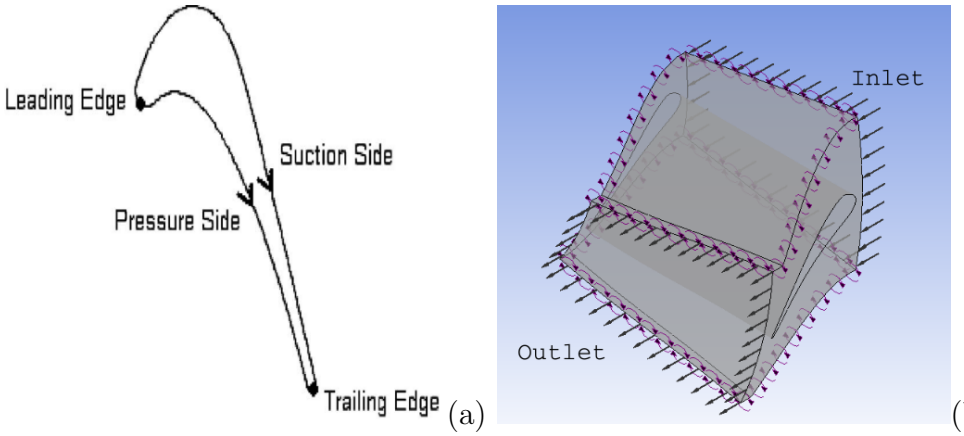

Figure 4.10: (a) Blade profile (Chitrakar et al., 2014) (b) Computational flow domain

from 5 to 20. The decrease in velocity could be atributted to the increase in pressure since they are inversely proportional and is consistent with what is expected in fluid flow (Acharya & Mahmood, 2006), (Jaeger, 2014).

Shown in Figure 4.15 is velocity contours across the turbine flow path at turbine inlet temperature of 600 K, 1,000 K, 1,400 K and 1,800 K respectively. The velocity at mid point of the suction side of the blade increased by 297% with increase in turbine inlet temperature from 600 K to 1,800 K. The increase in velocity with increase in turbine inlet temperature could be attributed to increase in kinetic energy of the fluid (Yamada & Asako, 2007).

4.4 Temperature Field

Shown in Figure 4.16 is temperature distribution across the turbine flow path at rotational speed of 3000 rpm, 6,000 rpm, 9,000 rpm and 12,000 rpm respectively. The upper rotational speed of 12,000 rpm was used since there was a significant change in temperature observed at that point. From the figure, temperature is seen to decrease with increasing rotational speed. Temperature decreased from inlet to outlet due to increase in velocity (Darshan et al., 2016). The temperature at mid point of the pressure side increased by 0.2% with

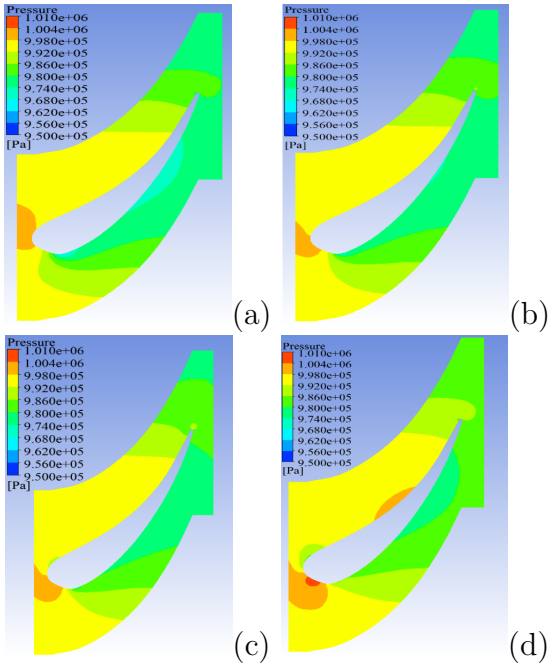

Figure 4.11: Pressure distribution at (a) 3,000 rpm, (b) 6,000 rpm, (c) 9,000 rpm and (d) 12,000 rpm

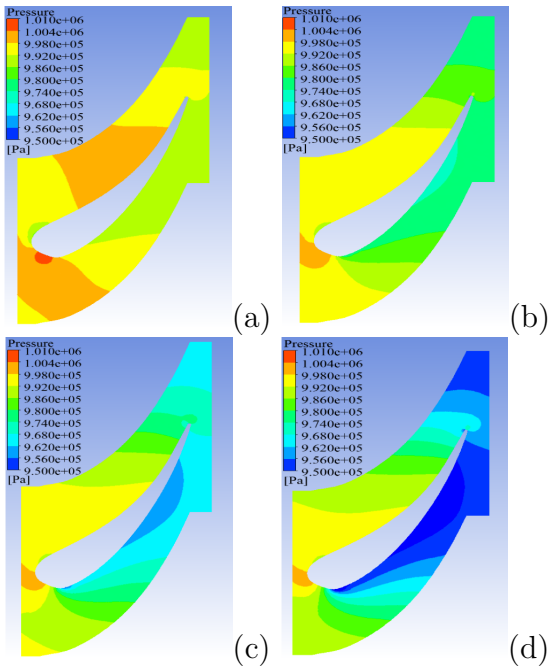

Figure 4.12: Pressure distribution at (a) 600 K, (b) 1000 K, (c) 1400 K and (d) 1800 K

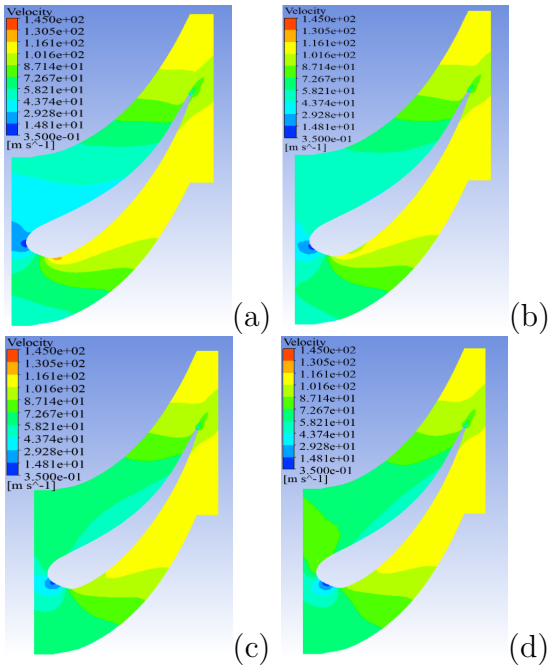

Figure 4.13: Velocity distribution at (a) 3000 rpm, (b) 6000 rpm, (c) 9000 rpm and (d) 12000 rpm

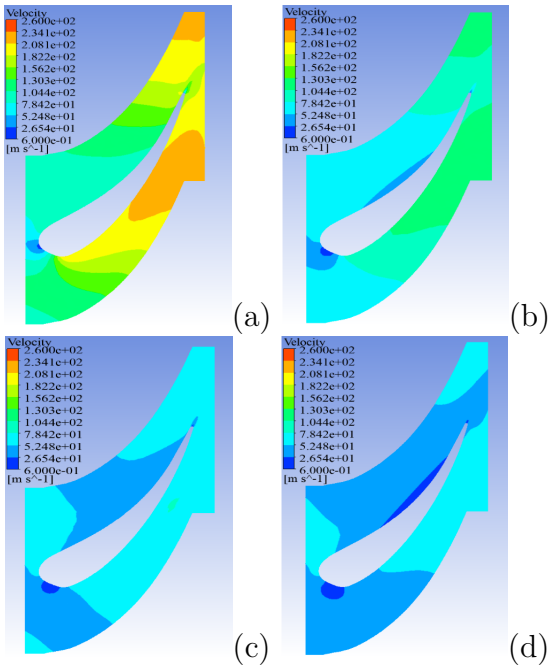

Figure 4.14: Velocity distribution at (a) 5, (b) 10, (c) 15 and (d) 20

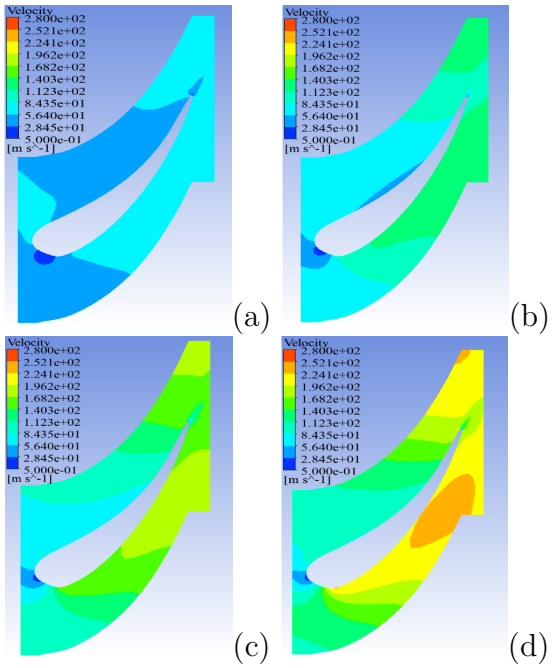

Figure 4.15: Velocity distribution at (a) 600 K, (b) 1,000 K, (c) 1,400 K and (d) 1,800 K

increase in rotational speed. That is due to fluid separation regions developed as the rotational speed increased. Figure 4.17 shows temperature distribution across the turbine flow path at pressure ratio of 5, 10, 15 and 20 respectively. The temperature increased with increase in pressure ratio. It can be attributed to pressure being directly proportional to temperature at constant volume as stated by Gay-Lussacs law in section 3.3. The pressure and temperature have a direct effect mass flow rate of syngas turbine (Johnson, 1991).

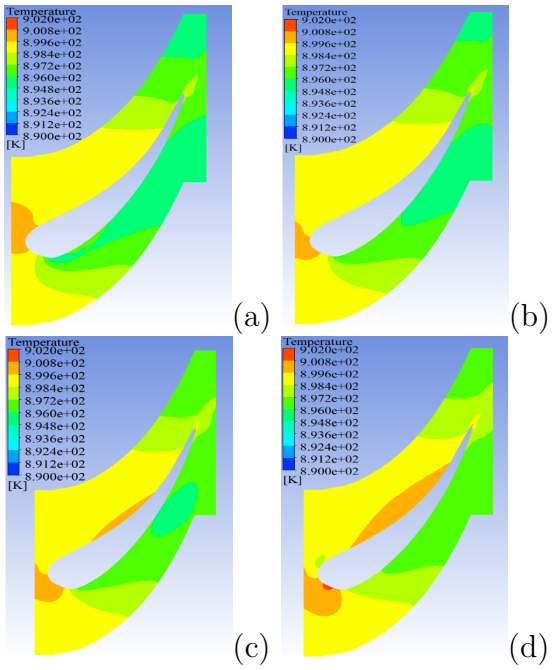

Figure 4.16: Temperature distribution at (a) 3,000 rpm, (b) 6,000 rpm, (c) 9,000 rpm and (d) 12,000 rpm

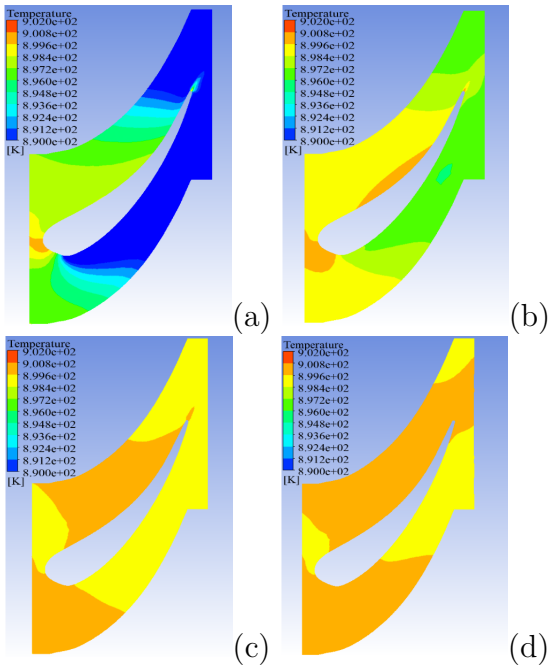

Figure 4.17: Temperature distribution at (a) 5, (b) 10, (c) 15 and (d) 20

4.5 Influence of Turbine Performance Parameters

4.5.1 Effect of Rotational Speed

Figure 4.18 shows the variation in power with increase in rotational speed. The maximum power for syngas combustion gases was 2.46 kW at a rotational speed of 11000 rpm. The power generated from Syngas combustion gases increased with increase in rotational speed by 108% and then decreased by 9%. The increase in power can be attributed to it's direct relationship with rotational speed as shown in Equation 3.9 in section 3.1 of methodology. However further increase in rotational speed resulted in flow mixing at the blade trailing edge causing increased entropy leading to reduced the power output(Bringhenti, Tomita, Silva, & Mendes Carneiro, 2015). The maximum power for natural gas combustion was 3.71 kW at a rotational speed of 13000 rpm. The natural gas combustion gases power also increased with increase in rotational speed by 148% and then decreased by 0.4%. There was a maximum difference of 63% between the syngas combustion power curve and natural gas combustion power. The difference in power was attributed to high heating values of natural gas at 50 MJ/kg and low heating values of syngas of 16 MJ/kg (Ghenai, 2010).

Figure 4.19 shows the variation in efficiency with increase in rotational speed. The maximum efficiency for syngas combustion was 92.71% at a rotational speed of 10000 rpm. The syngas combustion gases efficiency increased with increase in rotational speed by 13% and then decreased by 2%. The increase in efficiency with increased rotational speed was attributed to increasing power output which is proportional to angular velocity. Further increase in rotational speed resulted in decreased efficiency due to flow mixing at the blade trailing edge causing increased entropy (Bringhenti et al., 2015). The maximum efficiency for syngas combustion gases was 92.85% at a rotational speed of 12000

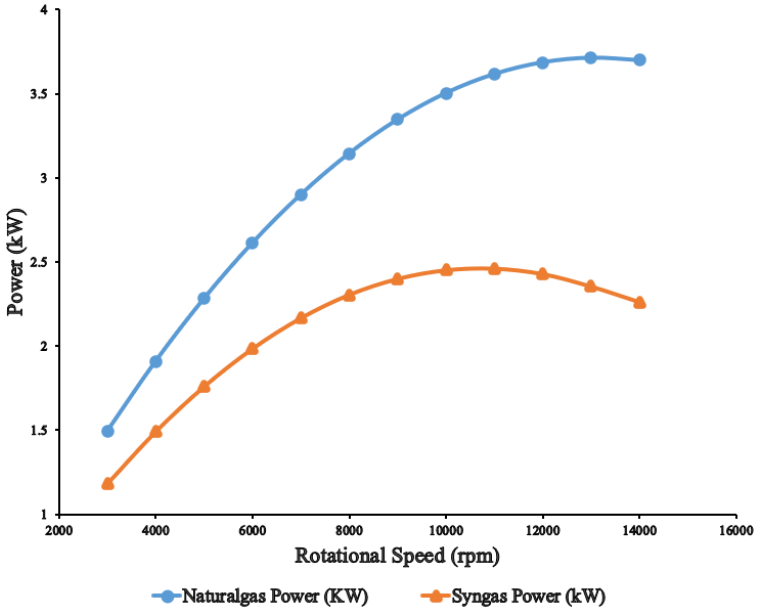

Figure 4.18: Variation in power with rotational speed

rpm. The natural gas combustion gases efficiency also increased with increase in rotational speed by 18% and then decreased by 0.13%. The difference in efficiecny was attributed to heating values of natural gas at 50 MJ/kg and syngas at 16 MJ/kg (and Petroleum, 2015). Power and efficiency are directly related yet from Figures 4.18 and 4.19 there was a difference due to entropy at the blade trailing edge caused by flow recirculation at high rotational speed.

4.5.2 Effect of Pressure Ratio

Pressure ratio (r_P) is a ratio of inlet and outlet pressure. Pressure ratio is critical in design of gas turbine since it is produced by the compressor and the turbine cannot exceed it. Figure 4.20 shows the variation of power with increase in pressure ratio. Power produced from syngas combustion was observed to decrease with increase in pressure ratio by 43%. The decrease in power with increase in pressure ratio can be attributed to increased compressor work to produce high pressure ratio (Besharati-Givi & Li, 2015). The power produced from natural gas combustion also decreased with increase in pressure ratio by

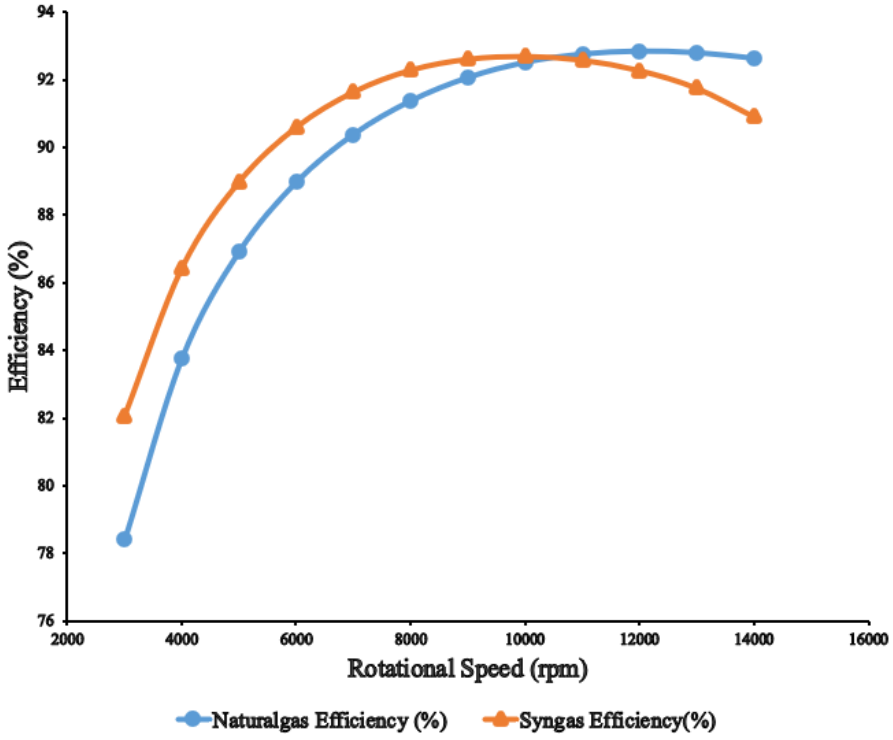

Figure 4.19: Variation in efficiency with rotational speed

54%. It is consistent with information in literature that power decreases with increase in pressure ratio at constant temperature (K. Ibrahim & Rahman, 2012). The difference in power was attributed to heating values of natural gas at 50 MJ/kg and syngas at 16 MJ/kg (Ghenai, 2010).

Shown in Figure 4.21 is the variation of efficiency with increase in pressure ratio. The syngas combustion efficiency increased with increase in pressure ratio by 4% and then decreased by 24%. The overall efficiency of a gas turbine increases with increase in pressure ratio at a given temperature up to a certain value then it starts decreasing, due to increased compressor load (K. Ibrahim & Rahman, 2012), (Boyce, 2002). The natural gas combustion gases efficiency increased with increase in pressure ratio by 6% and then decreased by 4%. The difference in efficiecny was attributed to heating values of natural gas at 50 MJ/kg and syngas at 16 MJ/kg (Ghenai, 2010).

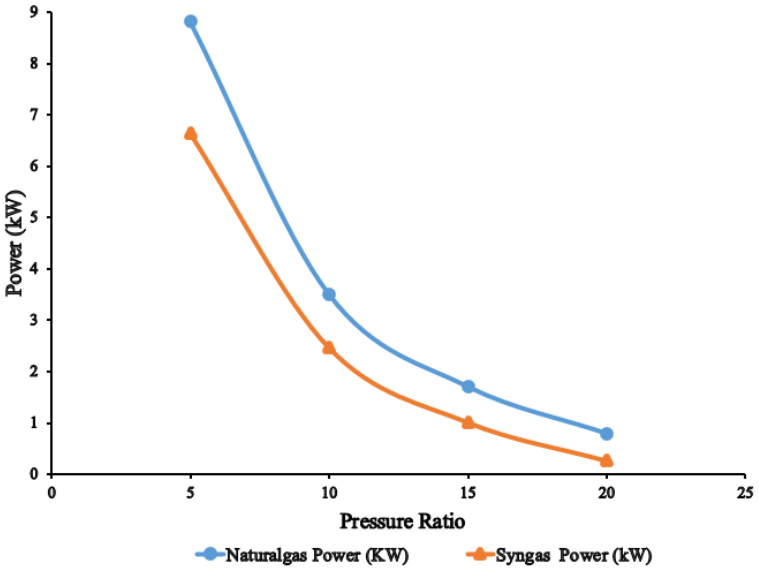

Figure 4.20: Variation in power with pressure ratio

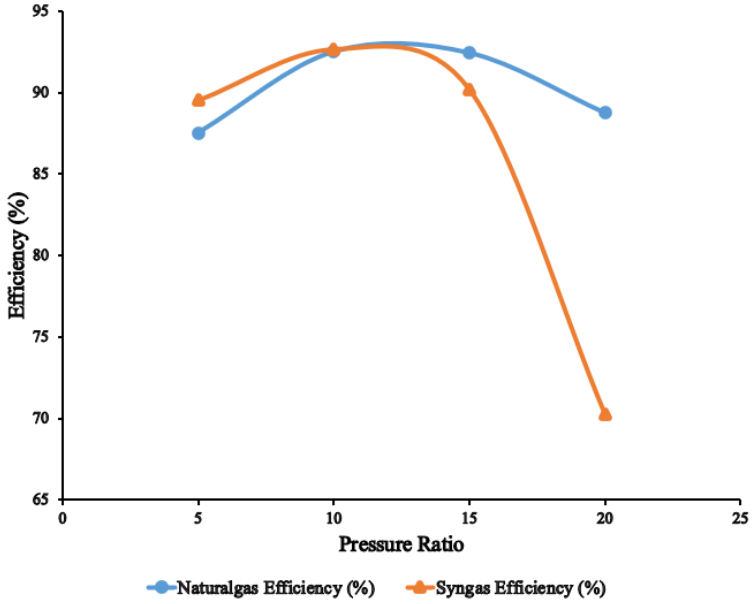

Figure 4.21: Variation in efficiency with pressure ratio

4.5.3 Effect of Turbine Inlet Temperature

Figure 4.22 shows variation in power with increase in turbine inlet temperature. Syngas combustion gases power increased with increase in turbine inlet temperature by 0.52%. This can be attributed to increase in turbine work output as turbine inlet temperature increased, since power is a product of work and mass flow rate (T. Ibrahim & Rahman, 2010). The natural gas combustion gases power increased with increase in turbine inlet temperature by 0.65%. The difference in power was attributed to heating values of natural gas at 50 MJ/kg and syngas at 16 MJ/kg (Ghenai, 2010).

Figure 4.23 shows the variation in efficiency with increase in turbine inlet temperature. The syngas combustion efficiency increased with increase in turbine inlet temperature by 1% and then decreased by 0.42%. Thermal efficiency of the turbine increased with increase in inlet temperature up to a maximum at 900 K. Further increase in turbine inlet temperature led to high turbine exit temeprature resulting in decreased thermal efficiency as shown by Equation 3.11. The natural gas combustion gases efficiency increased with increase in turbine inlet temperature by 0.5% and then decreased by 0.55%. At 1800 K the efficiency of natural gas combustion is lower than that of syngas due to high exit temperature. The difference in efficiency was attributed to heating values of natural gas at 50 MJ/kg and syngas 16 MJ/kg (Ghenai, 2010).

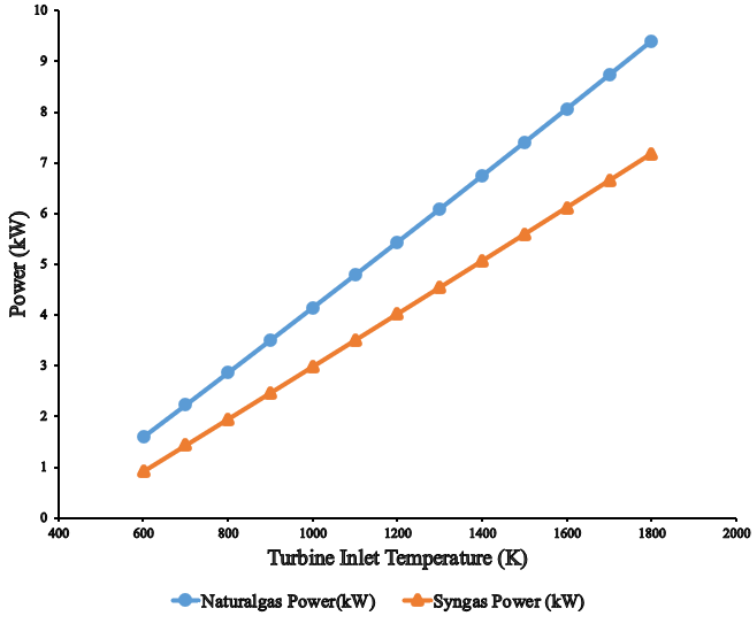

Figure 4.22: Variation in power with inlet temperature

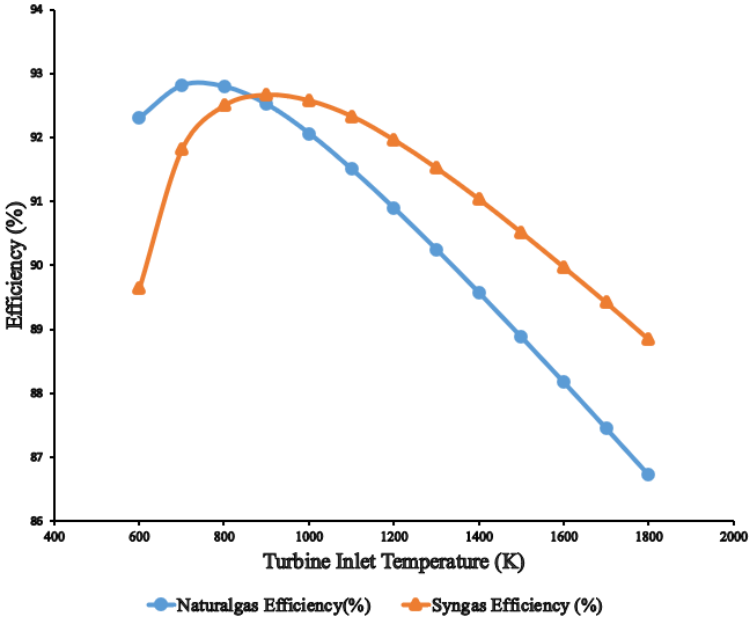

Figure 4.23: Variation in efficiency with inlet temperature

CHAPTER FIVE

CONCLUSIONS AND RECOMMENDATIONS

5.1 Conclusions

In this research, a numerical model of syngas expansion in gas turbine utilizing Mui basin coal was developed. A CFD model of gas turbine rotor was developed and validated using experimental data from literature. ANSYS CFX simulations were carried out to determine performance of syngas and natural gas combustion expansion in rotor model with varying parameters (rotational speed, pressure ratio and turbine inlet temperature).

Based on the findings of this research, following conclusions were made;

(a) The pressure and temperature distribution across computational domain showed regions of high pressure and turbulence at leading and trailing edge of the blade. This led to the conclusion that for blade life to be extended these regions require strengthening.

(b) The power produced by expansion of natural gas combustion gases in turbine rotor was 41% more than that of syngas combustion gases which was attributed to high heating value of natural gas. This led to the conclusion that further improved combustion processes through conducting optimization simulation should be done.

(c) The efficiency of rotor increased with increase in rotational speed up to a maximum of 92.7%. Further increase in rotational speed led to decrease in efficiency which was due to turbulence at the blade trailing edge leading to the conclusion that syngas turbines would be just as effective as natural gas turbines particularly at speeds below 10,000 rpm.

(d) The efficiency of rotor increased with increase in turbine inlet temperature up to a maximum of 92.7% at 900 K and then started decreasing due to increased heat loss. It can be concluded that for rotor model highest temperature for maximum efficiency is 900 K for both syngas and natural gas.

5.2 Recommendations

From this research and results discussions, the following recommendations for later study are suggested:

(a) The main syngas combustion products are water and carbon dioxide, moisture reduces blade life. Further work is required on an upgrading technique to remove water.

(b) The effect of rotational speed on performance of turbine rotor was evaluated, however blade cooling was not carried out due to limitations of the computer processor used. Further studies can be done on performance of a cooled turbine blade with varying rotational speed.

(c) Simulation model developed can be scaled up to construct a gas turbine for use with lignite coal from Mui basin.

REFERENCES

Abbasi, S., & Gholamalipour, A. (2019). Parametric study of injection from the casing in an axial turbine. *Proceedings of the Institution of Mechanical Engineers, Part A: Journal of Power and Energy*, *0*(0), 1–12. doi: 10 .1177/0957650919877276

Abdelfattah, S. A., Chibli, H. A., & Schobeiri, M. T. (2011). Aerodynamic Investigation of the Performance of a Two Stage Axial Turbine At Design and Off-Design Conditions. *Proceedings of ASME Turbo Expo 2011*. Retrieved from `http://abdelfattah2011.pdf` doi: 10.1115/ GT2011-45909

Acharya, S., & Mahmood, G. (2006). Turbine Blade Aerodynamics. *Mechanical Engineering*, *1*(225), 364–380.

Africa, U. K., & East. (2016). Development of Kenya's Power Sector 2015-2020.

Agarwal, S., Kachhwaha, S., & Mishra, R. (2012). Performance Improvement of a Regenerative Gas Turbine Cycle Through Integrated Inlet Air Evaporative Cooling and Steam Injection. *International Journal of Emerging Technology and Advanced Engineering*, *2*(12), 354–363. Retrieved from `http://www.ijetae.com/files/Volume2Issue12/IJETAE{\%}7B{\_}{\%}7D1212{\%}7B{\_}{\%}7D65.pdfhttp://www.ijetae.com/files/Volume2Issue12/IJETAE{\_}1212{\_}65.pdf`

AGECC. (2010). *Energy for a Sustainable Future* (Tech. Rep. No. April). doi: DOI:10.1016/j.enbuild.2006.04.011

Agrawal, R. K. (2000). Coal Gasification. In *Energy and power generation handbook* (chap. 20).

Ainley, D. G., & Mathieson, G. C. R. (1951). An Examination of the Flow and Pressure Losses in Blade Rows of Axial-Flow Turbines.

, *2891*(2891), 1–33. Retrieved from http://scholar.google.com/scholar?hl=en{\&}btnG=Search{\&}q=intitle:An+Examination+of+the+Flow+and+Pressure+Losses+in+Blade+Rows+of+Axial-Flow+Turbines{\#}0

Alday, L. F., Fluder, M., & Sparks, J. (1973). The Numerical Computation of Turbulent Flows. *Journal of High Energy Physics*, *1974*(10), 269–289. doi: 10.1007/JHEP10(2012)057

Al-hadhrami, L. M., Shaahid, S. M., & Al-mubarak, A. A. (2011). Jet Impingement Cooling in Gas Turbines for Improving Thermal Efficiency and Power Density.

Ali, L. S., Mohammed, H., & Kamel, H. M. (2017). The Number of Blade Effects on the Performance of a Mixed Turbine Rotor. , *37*(3), 349–360.

Almarzooq, Y. (2014). Gas Turbine. , 333–365.

Almasi, A. (2015). Advanced gas turbine packaging. *Australian Journal of Mechanical Engineering*, *13*(1). Retrieved from http://www.engineersmedia.com.au/journals/ajme/2015/13{_}1/M12{_}091.html doi: 10.7158/M12-091.2015.13.1

Aminov, R. Z., Moskalenko, A. B., & Kozhevnikov, A. I. (2018). Optimal gas turbine inlet temperature for cyclic operation. *Journal of Physics*. doi: 10.1088/1742-6596/1111/1/012046

and Petroleum, M. o. E. (2015). Draft National Energy and Petroleum Policy.

Aneke, M., & Wang, M. (2017). Thermodynamic Comparison of alternative Biomass Gasification Techniques for producing Syngas for Gas Turbine Application. *Energy Procedia*, *142*, 829–834. Retrieved from https://doi.org/10.1016/j.egypro.2017.12.133 doi: 10.1016/j.egypro.2017.12.133

Arabnia, M., Sivashanmugam, V. K., & Ghaly, W. (2011). Optimization of an Axial Turbine Rotor for High Aerodynamic Inlet. *Proceedings of ASME Turbo Expo 2011*. doi: 10.1115/GT2011-46757

Arnone, A., Bonaiuti, D., Focacci, A., Pacciani, R., Scotti, A., Greco, D., & Spano, E. (2004). Parametric Optimization of a High–Lift Turbine Vane. In *Proceedings of asme turbo expo, power for land, sea, and air.*

ASME. (2007). The World's First Industrial Gas Turbine Set – GT Neuchâtel a Historic Mechanical Engineering Landmark.

Aubé, M., & Hirsch, C. (2001). Numerical Investigation of a 1-1/2 Axial Turbine Stage at Quasi-Steady and Fully Unsteady Conditions. *Volume 1: Aircraft Engine; Marine; Turbomachinery; Microturbines and Small Turbomachinery*, V001T03A013. Retrieved from `http://proceedings.asmedigitalcollection.asme.org/proceeding.aspx?doi=10.1115/2001-GT-0309` doi: 10.1115/2001-GT-0309

Ayong Le Kama, A., Fodha, M., & Lafforgue, G. (2013). Optimal Carbon Capture and Storage Policies. *Environmental Modeling and Assessment*, *18*(4), 417–426. doi: 10.1007/s10666-012-9354-y

Bari, P., David, V. R., Torresi, M., Fortunato, B., & Camporeale, S. M. (2014). Design of an Axial Impulse Turbine for Enthalpy Drop Recovery. *Turbine Technical Conference and Exposition*, 1–12.

Barnes, I. (2013). *Recent Operating Experience And Improvement Of Commercial IGCC, CCC/222*.

Bathie, W. (1996). *Fundamentals of Gas Turbines* (2nd ed.). John Wiley & Sons, Inc.

Baturin, O., Popov, G., Novikova, J., Kolmakova, D., & Volkov, A. (2017). Strength and Gas Dynamic Methods of Development 0f Axial Turbine Turbocharger. *International Conference on Mechanical, System and Control Engineering, ICMSC*, 44–47. doi: 10.1109/ICMSC.2017.7959440

Bayoumy, A. H., Nada, A. A., & Megahed, S. M. (2012). A Continuum Based Three-Dimensional Modeling of Wind Turbine Blades. *Journal of Computational and Nonlinear Dynamics*, *8*(3), 031004. Retrieved from

http://computationalnonlinear.asmedigitalcollection.asme.org/article.aspx?doi=10.1115/1.4007798 doi: 10.1115/1.4007798

Behr, T., Kalfas, A. I., & Abhari, R. A. (2006). Unsteady Flow Physics and Performance of a One-and-1/2-Stage Unshrouded High Work Turbine. In *Asme turbo expo 2006: Power for land, sea and air.*

Besharati-Givi, M., & Li, X. (2015). Impact of Blade Cooling on Gas Turbine Performance under Different Operation Conditions and Design Aspects. In *Asme power conference power san diego, california* (pp. 1–9).

Bhargava, R., Bianchi, M., De Pascale, A., Negri di Montenegro, G., & Peretto, A. (2007). Gas Turbine Based Power Cycles - A State-of-the-Art Review. *Power Engineering Conference*, 11.

Bhatt, M. S. (2012). Hybrid Clean Energy Technologies for Power Generation from Sub-Bituminous Coals: A Case of 250 MW Unit. *International Journal of Sustainable Energy*, *6451*(March), 1–14. doi: 10.1080/14786451.2011.631011

Bijak-Bartosik, E., Elsner, W., & Wysocki, M. (2009). Evolution of the wake in a turbine blade passage. *JOURNAL OF THEORETICAL AND APPLIED MECHANICS*, *47*(1), 41–53. Retrieved from http://www.ptmts.org/Bijak-Bart-Elsn-Wys-1-09.pdf

Binder, N., Carbonneau, X., & Chassaing, P. (2008). Off-Design Considerations through the Properties of Some Pressure-Ratio Line of Radial Inflow Turbines. *International Journal of RotatingMachinery*. doi: 10.1155/2008/273296

Boselli, P., & Zangeneh, M. (2011). An Inverse Design Based Methodology for Rapid 3D Multi-Objective/Multidisciplinary Optimization of Axial Turbines. *Volume 7: Turbomachinery, Parts A, B, and C*, 1459–1468. Retrieved from http://proceedings.asmedigitalcollection.asme.org/proceeding.aspx?articleid=1633997{\&}resultClick=1 doi: 10.1115/GT2011-46729

Boulle, M. (2019). The Hazy Rise of Coal in Kenya: The Actors, Interests and Discursive Contradictions Shaping Kenya's Electricity Future. *Energy Research and Social Science*, *56*(June). Retrieved from https://doi.org/10.1016/j.erss.2019.05.015 doi: 10.1016/j.erss.2019.05.015

Boyce, M. P. (2002). *GasTurbine Engineering Handbook* (2nd ed.). gulfProfrssional Publishing.

BP. (2020). *Statistical Review of World Energy 2020* (Tech. Rep.). Retrieved from https://www.bp.com/content/dam/bp/business-sites/en/global/corporate/pdfs/energy-economics/statistical-review/bp-stats-review-2020-full-report.pdf

Brar, J. S., Singh, K., Wang, J., & Kumar, S. (2012). Cogasification of Coal and Biomass: A Review. *International Journal of Forestry Research*, *2012*, 1–10. doi: 10.1155/2012/363058

Brdar, R. D., & Jones, R. M. (2000). IGCC Technology and Experience with Advanced Gas Turbines. *GE Power Systems*.

Breault, R. W. (2010). Gasification Processes Old and New: A Basic Review of the Major Technologies. *Energies*, *3*(2), 216–240. doi: 10.3390/en3020216

Bringhenti, C., Tomita, J. T., Silva, F. D. A., & Mendes Carneiro, H. F. D. F. (2015). One-Stage Power Turbine Preliminary Design and Analysis. *Journal of Aerospace Technology and Management*, *7*(2), 157–169. doi: 10.5028/jatm.v7i2.361

Bwana, S. O. (2021). *The Kenya Coal Report* (Tech. Rep.).

Cabot, G., Calbry, M., Xavier, P., Vandel, A., de Persis, S., Pillier, L., ... Favre, E. (2014). Effect of Carbon Capture on Combined Cycle Gas Turbine Efficiency Using Membrane Separation, EGR and OEA Effects on Combustion Characteristics. *Proceedings of ASME Turbo Expo 2014: Turbine Technical Conference and Exposition: GT2014: June 16 – 20, 2014, Düsseldorf, Germany*(February 2016), 1–10.

Carbo, M. C., Jansen, D., Dijkstra, J. W., van Buijtenen, J. P., & Verkooijen, A. H. M. (2009). Pre-Combustion Decarbonisation in IGCC: Gas Turbine Operating Window at Variable Carbon Capture Ratios. *Energy Procedia*, *1*(1), 669–673. Retrieved from http://dx.doi.org/10.1016/j.egypro.2009.01.088 doi: 10.1016/j.egypro.2009.01.088

Cerri, G., Chennaoui, L., & Mazzoni, S. (2014). Expander Models for a Generic 300 Mw F Class Gas Turbine for IGCC. , 1–10.

Chang, D., & Tavoularis, S. (2009). Unsteady Vortices and Blade Loading in a High-Pressure Turbine. *ASME Conference Proceedings*(48883), 1543–1552. Retrieved from http://link.aip.org/link/abstract/ASMECP/v2009/i48883/p1543/s1 doi: 10.1115/GT2009-59189

Chang, D., & Tavoularis, S. (2011). Effect of the Axial Spacing Between Vanes and Blades. *Proceedings of ASME Turbo Expo 2011*, 1–12.

Chitrakar, S., Baidar, B., & Koirala, R. (2014). Spanwise re-stacking techniques in turbo-machinery blades and application in Francis runner. , *4*(September).

Chyu, M. K., Mazzotta, D. W., Siw, S. C., Karaivanov, V. G., Slaughter, W. S., & Alvin, M. A. (2009). Aerothermal Challenges in Syngas, Hydrogen-Fired, and Oxyfuel Turbines-Part I: Gas-Side Heat Transfer. *Journal of Thermal Science and Engineering Applications*, *1*(1), 11002–1–11002–8. doi: 10.1115/1.3159479

Chyu, M. K., Siw, S. C., Karaivanov, V. G., Slaughter, W. S., & Alvin, M. A. (2009). Aerothermal Challenges in Syngas, Hydrogen-Fired, and Oxyfuel Turbines-Part II: Effects of Internal Heat Transfer. *Journal of Thermal Science and Engineering Applications*, *1*(1), 11003–1–11003–10. doi: 10.1115/1.3159480

Commission, E. R. (2019). *Terms of Reference for the Governance Committee* (Tech. Rep.). Retrieved from https://www.td.com/document/PDF/investor/2018/E-2018-Proxy-Circular.pdf

Conner, M. (2003). Sir Frank Whittle. *Power*, 1–6.

Cuciumita, C. F., Vilag, V. A., Silivestru, V., & Porumbel, I. (2012). Genetic Algorithm for Gas Turbine Blading Design. *Proceedings of the Asme Turbo Expo 2011, Vol 7, Pts a-C*, 1351–1361. doi: 10.1115/GT2011-46171

Daggupati, S., Mandapati, R. N., Mahajani, S. M., Ganesh, A., Pal, A. K., Sharma, R. K., & Aghalayam, P. (2011). Compartment modeling for flow characterization of underground coal gasification cavity. *Industrial and Engineering Chemistry Research*, *50*(1), 277–290. doi: 10.1021/ie101307k

Darshan, M. K., Annigeri, A., & Kumar, B. M. S. (2016). Numerical Analysis of Effect of Thermal Performance of Gas Turbine Nozzle guide vane. *International Journal of Engineering Research and Advanced Technology (IJERAT)*, *2*(01), 488–494.

Das, L. G., Samanta, P., & Murmu, N. C. (2013). An Investigation On Performance Characteristics of Radial In- Flow Turbo-Expander with Backswept Curved Rotor. , *3*(5), 229–234.

De Maesschalck, C., Lavagnoli, S., Paniagua, G., & Vinha, N. (2014). Aerothermodynamics of Tight Rotor Tip Clearance Flows in High-Speed Unshrouded Turbines. *Applied Thermal Engineering*, *65*(1-2), 343–351. Retrieved from `http://dx.doi.org/10.1016/j.applthermaleng.2014.01.015` doi: 10.1016/j.applthermaleng.2014.01.015

de Mello, P. E. B., Scuotto, S., Ortega, F. d. S., & Donato, G. H. B. (2014). Influence of Turbine Inlet Temperature on the Efficiency of Externally Fired Gas Turbines. In (chap. 6).

Dennis, R. A., Shelton, W. W., & Le, P. (2007). Development of baseline performance values for turbines in existing IGCC applications. , *2*, 1017–1049. Retrieved from `http://www.scopus.com/inward/record.url?eid=2-s2.0-34548715888{\&}partnerID=40{\&}md5=`

71defd85ec1f3d055f6031f73a3f57bd doi: 10.1115/GT2007-28096

Dongre, D., Vikas, T., & Vishal, R. (2014). Design and Analysis for Internal Cooling of Gas Turbine Blade. *International Journal For Engineering Applications and Technology*.

Du, J., Lin, F., Zhang, H., & Chen, J. (2008). Numerical simulation on the effect of tip clearance size on unsteadiness in tip clearance flow. *Journal of Thermal Science*, *17*(4), 337–342. doi: 10.1007/s11630-008-0337-x

Dubitsky, O., Weidermann, A., Nakano, T., & Perera, J. (2003). The Reduced Order Through-Flow Modeling of Axial Turbomachinery. *International Gas Turbine Congress IGTC*, *3*, 1–8. Retrieved from http://nippon.zaidan.info/seikabutsu/2003/00916/pdf/igtc2003tokyo{_}ts052.pdf

E4tech. (2009). Review of Technologies for Gasification of Biomass and Wastes. *Biomass*(June), 125. Retrieved from http://www.nnfcc.co.uk/tools/review-of-technologies-for-gasification-of-biomass-and-wastes-nnfcc-09-008 doi: 10.1016/j.dsr2.2004.06.026

Eifel, M., Caspary, V., Hönen, H., & Jeschke, P. (2009). Analysis of Internal Cooling Geometry Variations in Gas Turbine Blades. *Journal of Thermal Science*, *18*(4), 289–293. Retrieved from http://link.springer.com/10.1007/s11630-009-0289-9 doi: 10.1007/s11630-009-0289-9

Ekkad, S. (2001). Recent Development in Turbine Blade Film Cooling. , *7*(1), 21–40.

El-Batsh, H. M., & Bassily Hanna, M. (2011). An investigation on the effect of endwall movement on the tip clearance loss using annular turbine cascade. *International Journal of Rotating Machinery*, *2011*. doi: 10.1155/2011/489150

El-Batsh, H. M., Nada, S. A., Abdo, S. N., & El-Tayesh, A. A. (2013). Effect of secondary flows on heat transfer of a gas turbine blade. *International Journal of Rotating Machinery*, *2013*. doi: 10.1155/2013/797841

Elmekawy, A. N. (2018). Introduction to ANSYS Meshing Module 3 : Global Mesh Controls.

Emun, F., Gadalla, M., Majozi, T., & Boer, D. (2010). Integrated gasification combined cycle (IGCC) process simulation and optimization. *Computers and Chemical Engineering*, *34*(3), 331–338. Retrieved from `http://dx.doi.org/10.1016/j.compchemeng.2009.04.007` doi: 10.1016/j.compchemeng.2009.04.007

Energy Information Administration, U. S. (2022). IEO2021 Issues in Focus : Uncertainty in Coal Trade in India and Greater Southeast Asia. (February).

Energy Regulatory Commission. (2013). Updated Least Cost Power Development Plan. Period 2013-2033. (March).

Energy Regulatory Commission. (2014). Power Sector Medium Term Plan 2015-2020. , *21*(21).

Engineering, M., Engineering, M., & Engineering, M. (2011). Design of an Axial Turbine and Thermodynamic Analysis and Testing of a K03 Turbocharger. *Zuniga, Yoshio Samaizu Perez*.

Ennil, A. S. B., & Mahmouda, S. (2015). Optimization of Small Scale Axial Air Turbine Using Ansys CFX. In *Proceedings of 22nd theiier international conference, london, united kingdom.*

Espanani, R., Ebrahimi, S. H., & Ziaeimoghadam, H. R. (2013). Efficiency Improvement Methods of Gas Turbine. *Energy Environ. Eng.*, *1*(2), 36–54. Retrieved from `http://www.hrpub.org` doi: 10.13189/eee.2013.010202

Estrada, C. a. (2007). New Technology Used in Gas Turbine Blade Materials . *Scienctia et Technica Año XIII*(36), 297–301.

Etsap, I. E. a., & Brief, T. (2010). Syngas Production from Coal. *Technology*(May), 1–5.

Eunice, A.-B. (2014). *Gas Turbine Engine Turbine Blade Airfoil Profile*

Cross-Reference (No. 12).

Fantozzi, F., Desideri, U., De Prosperis, R., & Russo, A. (2010). Gas turbines fired with biomass pyrolysis syngas: Analysis of the overheating of hot gas path components. *Journal of Engineering for Gas Turbines and Power*, *132*(6), 1–8. doi: 10.1115/1.4000134

Farahani, A. S., & Kermani, M. J. (2014). *Modeling of Tip Leakage Losses in Axial Flow Turbines.*

Fareeza, N., Tan, E. S., Kumaran, P., Indra, T. M., Fadzilah, N., & Yoshikawa, K. (2016). Evaluating the Effect of Syngas Composition on Micro gas turbine Performance. *IOP Conference Series: Earth and Environmental Science*, *32*(1). doi: 10.1088/1755-1315/32/1/012042

Fossum, M., & V. Beyer, R. (1998). *Technical Report : Co-combustion: Biomass Fuel Gas and Natural Ga* (Tech. Rep.). SINTEF Energy Research.

Gambini, M., & Vellini, M. (2016). *Turbomachinery Fundamentals, Selection and Preliminary Design*. Retrieved from `http://link.springer.com/10.1007/978-3-662-48465-4`

Ganjikunta P.E, J. (2015). Design Considerations for Syngas Turbine Power Plants. , 1–10.

Gao, J., Zheng, P. Q., Dong, P., & Zha, X. (2014). Control of tip leakage vortex breakdown by tip injection in unshrouded turbines. *Journal of Propulsion and Power*, *30*(6), 1510–1519. doi: 10.2514/1.B35283

Gao, J., Zheng, Q., Liu, Y., & Dong, P. (2016). Effects of Blade Rotation on Axial Turbine Tip Leakage Vortex Breakdown and Loss. *Proceedings of the Institution of Mechanical Engineers, Part G: Journal of Aerospace Engineering*, *0*(0), 1–16. Retrieved from `http://pig.sagepub.com/lookup/doi/10.1177/0954410016656879` doi: 10.1177/0954410016656879

Gao, J., Zheng, Q., Liu, Y., & Zhao, Z. (2014). Reduction of turbine

tip clearance losses at design and off-design incidences by non-uniform tip injection. *Proceedings of the Institution of Mechanical Engineers, Part A: Journal of Power and Energy*, *228*(8), 889–902. doi: 10.1177/0957650914542455

Gao, Z., Narzary, D., Mhetras, S., & Han, J. C. (2007). Effect of inlet flow angle on gas turbine blade tip film cooling. *Journal of Turbomachinery*, *131*(3). doi: 10.1115/1.2987235

Gardner, W. B. (1979). *Energy Efficient Engine High-Pressure Turbine Uncooled Rig Technology Report* (Tech. Rep.).

Gas, T. (2008). Syngas in the Modern Energy Mix.

GE Power. (2016). Powering the World with Gas Power Systems.

Georgiadis, N., Yoder, D., & Engblom, W. (2006). Evaluation of Modified Two-Equation Turbulence Models for Jet Flow Predictions. *AIAA journal*(January), 1–16. Retrieved from `http://arc.aiaa.org/doi/pdf/10.2514/1.22650` doi: 10.2514/1.22650

Ghenai, C. (2010). Combustion of Syngas Fuel in Gas Turbine Can Combustor. *Advances in Mechanical Engineering*. doi: 10.1155/2010/342357

Giauque, A. (2015). Turbomachinery Aero-Thermodynamics. (February).

Giel, W., Bunker, S., Fossen, G. J. V., & Boyle, J. (2000). Heat Transfer Measurements Generation and Predictions Blade on a Power. (April).

Glenny, R. J. E., Northwood, J. E., & Smith, a. B. (2013). Materials for Gas Turbines. *International Materials Reviews*, *20*(1), 1–28. doi: 10.1179/095066075790136925

Gonzalo, J., Marín, A., Andrés, D., Zuluaga, H., Alberto, J., & Monroy, C. (2015). Comparison and Validation of Turbulence Models in the Numerical Study of Heat Exchangers. , *10*(19), 49–60.

Gorla, R. S. R., & Khan, A. a. (2003). Axial Flow and Radial Flow Gas Turbines. *Turbomachinery: Design and Theory*(1).

Guédez, R. (2011). Implementation and Validation of Loss Prediction Methods

to an Existing One Dimensional Axial Turbine Design Program.

Gupta, S., Chaube, A., & Verma, P. (2012). Review on Heat Transfer Augmentation Techniques: Application in Gas Turbine Blade Internal Cooling. *Journal of Engineering Science and Technology Review*, *5*(1), 57–62.

Hagos, F. Y., Aziz, A. R. A., & Sulaiman, S. A. (2014). Trends of Syngas as a Fuel in Internal Combustion Engines. *Advances in Mechanical Engineering*. doi: 10.1155/2014/401587

Hamakhan, I. A., & Korakianitis, T. (2010). Aerodynamic performance effects of leading-edge geometry in gas-turbine blades. *Applied Energy*, *87*(5), 1591–1601. Retrieved from `http://dx.doi.org/10.1016/j.apenergy.2009.09.017` doi: 10.1016/j.apenergy.2009.09.017

Han, J.-C. (2004). Recent Studies in Turbine Blade Cooling. *International Journal of Rotating Machinery*, *10*(6), 443–457. doi: 10.1080/10236210490503978

Han, S., Han, B., Jin, P., & Goldstein, R. J. (2001). Numerical production of the flow field near the tip of a rotating turbine blade. *Inzhenerno-Fizicheskii Zhurnal*, *74*(4), 14–22.

Hanna, B., H., E.-B., Diab, M. R., & Abdelsamee, A. A. (2018). Effect of Gas Turbine Blade Tip Injection on the Flow Characteristics and the Distribution of Heat Transfer Coefficient over Blade Surface. In *2nd young researchers in egyptian universities conference.* Retrieved from `https://www.researchgate.net/publication/324138654`

Hillebrandt, W., & Kupta, F. (2009). An introduction to turbulence. *Lecture Notes in Physics*, *756*, 1–20. doi: 10.1007/978-3-540-78961-1_1

Hirano, K. (2005). Application of Eutectic Composites to Gas Turbine System and Fundamental Fracture Properties Up To 1700 Degrees Centigrade. *Journal of the European Ceramic Society*, *25*(8 SPEC. ISS.), 1191–1199. doi: 10.1016/j.jeurceramsoc.2005.01.003

Holt, N. A. (2003). Operating experience and improvement opportunities for coal-based IGCC plants. *Materials at High Temperatures*, *20*(1), 1–6. doi: 10.1179/mht.2003.001

Hong, G., Holmes, A. S., Heaton, M. E., & Pullen, K. R. (2003). Design, Fabrication and Characterization of an Axial-Flow Turbine for Flow Sensing. (June), 702–705.

Horbach, T., Schulz, A., & Bauer, H. (2010). Trailing Edge Film Cooling of Gas Turbine Airfoils – External Cooling Performance of Various Internal Pin Fin Configurations. *Proceedings of ASME Turbo Expo 2010: Power for Land, Sea and Air Proceedings*(mm), 1–12.

Hozhabr, A., Tahavvor, A., & Samimi, S. (2012). Numerical Simulation of Flow Field between Gas Turbine Blades, GE F9 Model. *4th Conference on Thermal Power Plants, CTPP 2012*.

Huang, D., Zhang, H., Weng, S., & Su, M. (2016). Modeling and Simulation of IGCC Considering Pressure and Flow Distribution of Gasifier. *Applied Sciences*, *6*(10), 292. Retrieved from `http://www.mdpi.com/2076-3417/6/10/292` doi: 10.3390/app6100292

Hunt, R. J. (2011). *The History of the Industrial Gas Turbine.*

Ibrahim, T., & Rahman, M. (2010). Effects of Operation Conditions on Performance of a Gas Turbine Power Plant. (December), 135–144.

Ibrahim, T. K., Mohammed, M. K., Al Doori, W. H. A., Al-Sammarraie, A. T., & Basrawi, F. (2019). Study of the Performance of the Gas Turbine Power Plants from the Simple to Complex Cycle: A Technical Review. *Journal of Advanced Research in Fluid Mechanics and Thermal Sciences*, *57*(2), 228–250.

Idahosa, U., Golubev, V. V., & Balabanov, V. O. (2006). An Automated Optimal Design of a Fan Blade Using an Integrated CFD/MDO Computer Environment. *Engineering Applications of Computational Fluid Mechanics*, *1*, 509–525. doi: 10.1080/19942060.2008.11015217

IEA. (2015). Energy and Climate Change. *World Energy Outlook Spec. Rep.*, 1–200. doi: 10.1038/479267b

Iea. (2015). Key World Energy Statistics 2015. *Statistics*, 82. Retrieved from http://www.oecd-ilibrary.org/energy/key-world-energy-statistics-2009{\%}7B{_}{\%}7D9789264039537-enhttp://www.oecd-ilibrary.org/energy/key-world-energy-statistics-2009{_}9789264039537-en doi: 10.1787/9789264039537-en

IEA. (2021). Net Zero by 2050 A Roadmap for the. , 222.

IEA: Directorate of Global Energy Economics. (2015). World Energy Outlook 2015. *International Energy Agency*, 726. Retrieved from http://www.worldenergyoutlook.org/ doi: 10.1787/weo-2014-en

Indrawan, N., Kumar, A., Moliere, M., Sallam, K. A., & Huhnke, R. L. (2020). Distributed Power Generation Via Gasification of Biomass and Municipal Solid Waste: A Review. *Journal of the Energy Institute*, *93*(6), 2293–2313. Retrieved from https://doi.org/10.1016/j.joei.2020.07.001 doi: 10.1016/j.joei.2020.07.001

Industries, M. H. (2015). High-efficiency Gas Turbine Development applying 1600 C class " J " Technology. , *52*(2), 2–9.

Institute of Economic Affairs (IEA). (2015). Situational Analysis of Energy Industry , Policy and Strategy for Kenya. , 77.

International Energy Agency. (2012). *Energy Policies of IEA Countries - The United Kingdom 2012 Review*. Retrieved from https://www.iea.org/publications/freepublications/publication/UK2012{\%}7B{_}{\%}7Dfree.pdfhttps://www.iea.org/publications/freepublications/publication/UK2012{_}free.pdf doi: 10.1787/9789264171497-en

Investigations, E., By, S., & Simulations, N. (2001). Experimental Investigations Supported By Numerical Simulations. *Test*, 1–11.

Jacobs, E. N., Ward, K. E., & Pinkerton, R. M. (1948). The Characteristics

of 78 Related Airfoil Sections from Tests in the Variable-Density Wind Tunnel.

Jaeger, T. D. (2014). Development of a CFD Simulation Methodology for Adjusting the Axial Turbine in a Turbocharger.

Jamshidi, R., & Mazzei, L. (2018). *CFD Modeling of Fluidized Beds*. Elsevier Inc. Retrieved from http://dx.doi.org/10.1016/B978-0-12-409547-2.13698-4 doi: 10.1016/b978-0-12-409547-2.13698-4

Joao, A. (2014). Fast aerodynamic design of a one-stage axial gas turbine in order to produce a 3D geometry ready for optimization. (October).

Johnson, M. S. (1991). Prediction of Gas Turbine On- and Off-Design Performance When Firing Coal-Derived Syngas. *Proceedings of the ASME Turbo Expo*, *3*(April). doi: 10.1115/91GT215

Jones, R. M., & Shilling, N. Z. (2003). IGCC Gas Turbines for Refinery Applications. *GE Power Systems*.

Joo, Y.-J., Kim, M.-Y., Park, S.-I., & Seo, D.-K. (2016). Performance Analysis of Gas Turbine for Large-Scale IGCC Power Plant. *KEPCO Journal on Electric Power and Energy*, *2*(3), 415–419. doi: 10.18770/kepco.2016.02.03.415

K. Ibrahim, T., & Rahman, M. M. (2012). Effect of Compression Ratio on Performance of Combined Cycle Gas Turbine. *International Journal of Energy Engineering*, *2*(1), 9–14. doi: 10.5923/j.ijee.20120201.02

Kadhim, H. T., & Rona, A. (2018). Design optimization workflow and performance analysis for contoured endwalls of axial turbines. *Energy*, *149*, 875–889. Retrieved from https://doi.org/10.1016/j.energy.2018.02.001 doi: 10.1016/j.energy.2018.02.001

Kaikko, J. (1998). *Performance Prediction of Gas Turbines by Solving a System of Non-Linear Equations*.

Kang, D. W., Kim, C. M., Lee, J. H., Kim, T. S., & Sohn, J. L. (2016). Performance Maximization of IGCC Plant Considering Operating

Limitations of a Gas Turbine and Ambient Temperature. *Journal of Mechanical Science and Technology*, *30*(5), 2397–2408. Retrieved from http://link.springer.com/10.1007/s12206-016-0450-9 doi: 10.1007/s12206-016-0450-9

Kariuki, D. W., & Kuria, J. M. (2021). Coal-Key Energy Resource for the Future in Kenya? A Review. *International Journal of Advanced Research*, *3*(1), 72–85. doi: 10.37284/ijar.3.1.319

Karpowitz, D. (2005). Bézier Curve Fitting Method for Existing Turbine Blade Design. *Journalof Applied Engineering Mathematics*, *1*(April), 3–6.

Kawabata, M., Kurata, O., Iki, N., Furutani, H., & Tsutsumi, A. (2012). Advanced Integrated Gasification Combined Cycle (A-IGCC) by Exergy Recuperation — Technical Challenges for Future Generations. *Journal of Power Technologies*, *92*(2), 90–100.

Kerester, A. (2014). Gasification Can Help Meet the World's Growing Demand for Cleaner Energy and Products. *Cornerstone*, *2*(3).

Kim, Y. S., Lee, J. J., Kim, T. S., & Sohn, J. L. (2011). Effects of syngas type on the operation and performance of a gas turbine in integrated gasification combined cycle. *Energy Conversion and Management*, *52*(5), 2262–2271. Retrieved from http://dx.doi.org/10.1016/j.enconman.2011.01.009 doi: 10.1016/j.enconman.2011.01.009

Kim, Y. S., Lee, J. J., Kim, T. S., Sohn, J. L., & Joo, Y. J. (2010). Performance analysis of a syngas-fed gas turbine considering the operating limitations of its components. *Applied Energy*, *87*(5), 1602–1611. Retrieved from http://dx.doi.org/10.1016/j.apenergy.2009.09.021 doi: 10.1016/j.apenergy.2009.09.021

Kiock, R., Lehthaus, F., Baines, N. C., & Sieverding, C. H. (1985). The transonic flow through a plane turbine cascade as measured in four european wind tunnels. *Proceedings of the ASME Turbo Expo*, *1*(April 1986). doi: 10.1115/85IGT44

Korakianitis, T., Rezaienia, M. A., Hamakhan, I. A., & Wheeler, A. P. S. (2013). Two- and Three-Dimensional Prescribed Surface Curvature Distribution Blade Design (CIRCLE) Method for the Design of High Efficiency Turbines, Compressors, and Isolated Airfoils. *Journal of Turbomachinery*, *135*(4), 041002. Retrieved from http://turbomachinery.asmedigitalcollection.asme.org/article.aspx?doi=10.1115/1.4007443 doi: 10.1115/1.4007443

Kosowski, K., Piwowarski, M., Stepien, R., & Włodarski, W. (2012). Design and Investigations of a Micro-Turbine Flow Part. In *Asme turbo expo* (Vol. 7100, pp. 1–8).

KPLC. (2017). The Kenya Power and Lighting Company Limited: Annual Report and Financial Statements 2016/2017. , 63. Retrieved from http://www.kplc.co.ke/img/full/4rNGlk21KXmA{_}KENYAPOWERANNUALREPORTFA.pdf doi: 10.1016/j.ijheatfluidflow.2009.05.002

Kumar, S., & Amano, R. S. (2014). Numerical and Experimental Investigation for Internal Cooling of Two Pass Gas Turbine Blades Channels Using Broken V Ribs. In *Proceedings of asme turbo expo 2014: Turbine technical conference and exposition gt2014* (pp. 1–12).

Kumar, S., & Singh, O. (2013). Performance Evaluation of Gas-Steam Combined Cycle Having Transpiration Cooled Gas Turbine. *Distributed Generation & Alternative Energy Journal*, *28*(2), 43–60. Retrieved from http://www.scopus.com/inward/record.url?eid=2-s2.0-84879755539{\%}7B{\&}{\%}7DpartnerID=tZOtx3y1http://www.scopus.com/inward/record.url?eid=2-s2.0-84879755539{\&}partnerID=tZOtx3y1 doi: 10.1080/21563306.2013.10677550

Kumar, S., & Singh, O. (2014). Enhancement of Combined Cycle Performance Using Transpiration Cooling of Gas Turbine Blades with Steam. *Journal*

of Mechanical Science and Technology, *28*(6), 2429–2437. doi: 10.1007/s12206-014-0536-1

Kurz, R., Meher-homji, C., & Brun, K. (2012). Gas Turbine Performance and Maintenance.

Lahmeyer International. (2016). Development of a Power Generation and Transmission Master Plan, Kenya. Medium Term Plan 2015-2030. , *I*(October).

Lancaster, D. (2005). The Math Behind Bezier Cubic Splines. *Http://Www.Tinaja.Com*, 1–5. Retrieved from `http://www.tinaja.com/glib/cubemath.pdf`

Launder, B. E., & Sharma, B. I. (1974). Application of the Energy-Dissipation Model of Turbulence to the Calculation of Flow Near a Spinning Disc. *Letters in Heat and Mass Transfer*, *1*(2), 131–137. doi: 10.1016/0094-4548(74)90150-7

Lazzaretto, A., & Toffolo, A. (2001). Analytical and Neural Network Models for Gas Turbine Design and Off-Design Simulation. *International Journal of Applied Thermodynamics*, *4*, 173–182. doi: 10.5541/IJOT.1034000078

Leach, K., Thulin, R., & Howe, D. (1982). *Energy Efficient Engine Turbine Intermediate Case and Low-Pressure Turbine Component Test Hardware Detailed Design Report* (Tech. Rep.).

Lee, C., Lee, S. J., & Yun, Y. (2007). Effect of Air Separation Unit Integration on Integrated Gasification Combined Cycle Performance and NOx Emission Characteristics. *Korean Journal of Chemical Engineering*, *24*(2), 368–373. doi: 10.1007/s11814-007-5047-7

Lee, J. C., Lee, H. H., Joo, Y. J., Lee, C. H., & Oh, M. (2014). Process simulation and thermodynamic analysis of an IGCC (integrated gasification combined cycle) plant with an entrained coal gasifier. *Energy*, *64*, 58–68. Retrieved from `http://dx.doi.org/10.1016/j.energy.2013.11.069` doi: 10.1016/j.energy.2013.11.069

Lee, M. C., Seo, S. B., Chung, J. H., Kim, S. M., Joo, Y. J., & Ahn, D. H. (2010). Gas turbine combustion performance test of hydrogen and carbon monoxide synthetic gas. *Fuel*, *89*(7), 1485–1491. Retrieved from http://dx.doi.org/10.1016/j.fuel.2009.10.004 doi: 10.1016/j.fuel.2009.10.004

Li, H.-D., He, L., Li, Y. S., & Wells, R. (2006). Blading Aerodynamics Design Optimization With Mechanical and Aeromechanical Constraints. *ASME Conference Proceedings*, *2006*(4241X), 1319–1328. Retrieved from http://link.aip.org/link/abstract/ASMECP/v2006/i4241X/p1319/s1{\%}5Cnhttp://li{_}bladingaerodynamicsdesign06.pdf doi: 10.1115/GT2006-90503

Li, W., Qiao, W. Y., Xu, K. F., & Luo, H. L. (2008). Numerical Simulation of Tip Clearance Flow Passive Control in Axial Turbine. *Journal of Thermal Science*, *17*(2), 147–155. doi: 10.1007/s11630-008-0147-1

Li, X. C., Subbuswamy, G., & Zhou, J. (2013). Performance of Gas Turbine Film Cooling with Backward Injection. *Energy and Power Engineering*, *2013*(July), 132–137. doi: 10.4236/epe.2013.54B025

Ling, Z., & Guoliang, W. (2011). Large Eddy Simulation on Compound Angle Film Cooling of Turbine Blades.

Liu, A., & Weng, Y. (2009). Effects of Lower Heat Value Fuel on the Operations of Micro-Gas Turbine. *Energy and Power Engineering*, *01*(01), 28–37. doi: 10.4236/epe.2009.11005

Lubbock, R. J., & Oldfield, M. L. (2018). Turbulent Velocity and Pressure Fluctuations in Gas Turbine Combustor Exit Flows. *Proceedings of the Institution of Mechanical Engineers, Part A: Journal of Power and Energy*, *232*(4), 337–349. doi: 10.1177/0957650917732885

Luo, J., Xiong, J., Liu, F., & McBean, I. (2010). Secondary Flow Reduction by Blade Redesign and Endwall Contouring Using an Adjoint Optimization Method. *ASME Conference Proceedings*, *2010*(44021), 547–562.

Retrieved from http://link.aip.org/link/abstract/ASMECP/v2010/i44021/p547/s1 doi: 10.1115/GT2010-22061

Majoumerd, M. M., Raas, H., Jana, K., De, S., & Assadi, M. (2017). Coal Quality Effects on the Performance of an IGCC Power Plant with CO2 Capture in India. *Energy Procedia*, *114*(1876), 6478–6489. Retrieved from http://dx.doi.org/10.1016/j.egypro.2017.03.1784 doi: 10.1016/j.egypro.2017.03.1784

Marn, A., Göttlich, E., Malzacher, F., & Pirker, H. (2009). The Effect of Rotor Tip Clearance Size onto the Separated Flow through a Super-Aggressive S-Shaped Intermediate Turbine Duct Downstream of a Transonic Turbine Stage. In *Asme turbo expo 2009: Power for land, sea and air* (pp. 1–15).

Matveev, I. B. (2011). Plasma or Retirement. Alternatives to the Coal-Fired Power Plants. *IEEE Trans. Plasma Sci.*, *39*(12 PART 1), 3259–3262. doi: 10.1109/TPS.2011.2135384

Matveev, V. N., Baturin, O. V., Popov, G. M., & Kolmakova, D. A. (2012). The Results of Gas Dynamic and Strength Improvement of Turbocharger TK-32 Axial Turbine.

Maurstad, O. (2005). An Overview of Coal Based Integrated Gasification Combined Cycle (IGCC) Technology. *MIT, Laboratory for Energy and the Environment*, 44. doi: 10.1533/9780857096180.129

Mazzotta, D. W., Chyu, M. K., & Alvin, M. A. (2007). Airfoil Heat Transfer Characteristics in Syngas and Hydrogen Turbines. *Proceedings of the ASME Turbo Expo*, *3*, 793–801. doi: 10.1115/GT2007-28296

Meher-Homji, C. Zachary, J., & A., B. (2010). Gas turbine fuel system design. Combustion and operability. *Proceedings of the Thirty-Ninth Turbomachinery Symposium*. Retrieved from http://turbolab.tamu.edu/proc/turboproc/T39/ch16{_}Meher-Homji.pdf

Meher-Homji, C. B. (2000). 'The Historical Evolution of Turbomachinery. *Proceedings of the 29th Turbomachinery ...*, 281–322. Retrieved from

http://turbo-lab.tamu.edu/proc/turboproc/T29/t29pg281.pdf

Menter, F. R. (1993). AIAA 93 · 2906 Zonal Two Equation k · co Turbulence Models for Aerodynamic Flows . Mailing Address : 24th Fluid Dynamics Conference FOR AERODYNAMIC FLOWS. *Fluid Dynamics*.

Menter, F. R. (1994). Two-Equation Eddy-Viscosity Turbulence Models for Engineering Applications. *AIAA Journal*, *32*(8), 1598–1605. Retrieved from http://arc.aiaa.org/doi/10.2514/3.12149 doi: 10.1016/0029-554X(80)90461-9

Miller, A., Pyzik, E., & Jarzebowski, S. (2012). Impact of Inlet Air Cooling on Gas Turbine Performance. *Journal of Power Technologies*, *92*(4), 249–257.

Miller, B. G. (2011). *U.S. and International Activities for Near-Zero Emissions during Electricity Generation*. doi: 10.1016/b978-1-85617-710-8.00011-x

Miller, B. G. (2017). *Clean Coal Technologies for Advanced Power Generation* (Vol. 5). doi: 10.1016/b978-0-12-811365-3.00006-5

Ministry of Energy and Petroleum, R. o. K. (2014). Strategic Plan 2013-2017.

Mobil Exxon. (2016). The Outlook for Energy: A View to 2040.

Monteiro, V. G., Zaparoli, E. L., de Andrade, C. R., & de Lima, R. C. (2012). Numerical Simulation of Performance of an Axial Turbine First Stage. *Journal of Aerospace Technology and Management*, *4*(2), 175–184. doi: 10.5028/jatm.2012.04025411

Morgese, G., Torresi, M., Fortunato, B., & Camporeale, S. M. (2015). Optimized Aerodynamic Design of Axial Turbines for Waste Energy Recovery. *Energy Procedia*, *82*, 194–200. doi: 10.1016/j.egypro.2015.12.019

Murugan, M., Ghoshal, A., Bravo, L., Xu, F., Hsu, M. C., & Bazilevs, Y. (2018). Articulating axial-flow turbomachinery rotor blade for enabling variable speed gas turbine engine. *2018 Joint Propulsion Conference*. doi: 10.2514/6.2018-4522

Nagpurwala, Q. H. (2012). Design of Axial Flow Turbine-3. *M S Ramaiah School of Advanced Studies, Bengaluru*, 1–42.

Nandakumar, N., & Moorthi, N. S. (2015). Performance Analysis of Gas Turbine Blade Cooling by CFD. , *1*(4), 3–9.

Narzary, D. P., Liu, K.-c., Rallabandi, A. P., & Han, J.-c. (2010). Influence of Coolant Density on Turbine Blade Film-Cooling Using Pressure Sensitive Paint Technique. In *Power for land, sea and air* (pp. 1–12).

Nayak, L. J., & Mahto, D. (2014). Effect of Gas Turbine Inlet Temperature on Combined Cycle Performance. (April). doi: 10.13140/2.1.2178.2089

Nemnem, A. F., Turner, M. G., Siddappaji, K., & Galbraith, M. (2014). A smooth curvature-defined meanline section option for a general turbomachinery geometry generator. *Proceedings of the ASME Turbo Expo*, *2B*(December 2016). doi: 10.1115/GT2014-26363

Nemnem, A. F., Turner, M. G., Siddappaji, K., & Galbraith, M. (2018). A Smooth Curvature-Defined Meanline Section Option for a General Turbomachinery Geometry Generator. , 1–20.

Ngugi, K. P. (2012). What Does Geothermal Cost? – The Kenya Experience. *Short Course VII on Exploration for Geothermal Resources.*, 1–13. Retrieved from `http://www.os.is/gogn/unu-gtp-sc/UNU-GTP-SC-14-13.pdf`

Niu, M., & Zang, S. (2009). Influences of tip cooling injection on tip clearance control at design and off-design incidences. *International Journal of Rotating Machinery*, *2009*. doi: 10.1155/2009/160423

Nowak, G., & Nowak, I. (2012). Shape Design of Internal Cooling Passages Within a Turbine Blade. *Engineering Optimization*, *44*(4), 449–466. Retrieved from `http://www.tandfonline.com/doi/abs/10.1080/0305215X.2011.580742` doi: 10.1080/0305215X.2011.580742

Nzove, S. N. (2021). *Development and Evaluation of Performance of a Bench Scale Gasifier for Sub-Bituminous Coal* (Unpublished doctoral

dissertation).

Office of Nuclear Regulatory Research. (2012). Computational Fluid Dynamics Best Practice Guidelines for Dry Cask Applications Draft Report for Comment.

of Kenya, R. (2018). *National Broadband Strategy 2018-2023* (Tech. Rep.).

Oluyede, E. O., & Phillips, J. N. (2006). Fundamental Impact of Firing Syngas in Gas Turbines. *Most*(January), 11. doi: 10.1115/GT2007-27385

Oluyede, E. O., & Phillips, J. N. (2007). Fundamental impact of firing syngas in gas turbines. *Proceedings of the ASME Turbo Expo*, *3*, 175–182. doi: 10.1115/GT2007-27385

Oyedepo, S. O., & Kilanko, O. (2014). Thermodynamic Analysis of a Gas Turbine Power Plant Modeled with an Evaporative Cooler. , *17*(1), 14–20. doi: 10.5541/ijot.480

Parasaram, R. K. N., & Charyulu, T. N. (2012). Airfoil Profile Design by Reverse Engineering Bezier Curve. *International Journal of Mechanical Engineering and Robotics Research*, *1*(3), 410–420.

Pathirathna, K. (2013). Gas Turbine Thermodynamic and Performance Analysis Methods Using Available Catalog Data. (October), 101.

Pillai, V. T., S, J. J., & Y, G. B. (2015). Numerical Investigation Effectiveness of Adiabatic film Cooling of Gas Turbine Blades. , *5*(7), 872–880.

Power, A., & Limited, C. (2016). 1,050MW Coal Fired Power Plant Stakeholder Engagement Plan. (July).

Qi, L., & Zhou, Y. (2014). Turbine Blade Tip Leakage Flow Control by Unsteady Periodic Wakes of Upstream Blade Row. *Procedia Engineering*, *80*, 202–205. Retrieved from `http://dx.doi.org/10.1016/j.proeng.2014.09.075` doi: 10.1016/j.proeng.2014.09.075

Rahman, M. H., Kim, S. I., Hassan, I., & Ayoubi, C. E. (2010). Unsteady Tip Leakage Flow Characteristics and Heat Transfer on Turbine Blade Tip and Casing. In *Asme turbo expo 2010: Power for land, sea and air* (pp.

1–10).

Rao, J. S., & Saravanakumar, M. (2008). Numerical Simulation of the Flow in a Two Stage Turbine Driving a Liquid Oxygen Pump. In *The 12th international symposium on transport phenomena and dynamics of rotating machinery* (pp. 1–7). doi: 10.15713/ins.mmj.3

Rao, V. (2014). Analytical Comparative Study of GAS Turbine Blade Materials Used In Marine Applications Using Fea Techniques. , *1*(1).

Razak, A. M. (2013). *Gas Turbine Performance Modelling, Analysis and Optimisation*. Woodhead Publishing Limited. Retrieved from http://dx.doi.org/10.1533/9780857096067.3.423 doi: 10.1533/9780857096067.3.423

Republic of Kenya. (2014). 10 Year Power Sector Expansion Plan 2014-2024. (June), 211.

Research, I. f. E. (2006). The Facts About Air Quality and Coal-Fired Power Plants. , 1–11.

Roach, P. J., & Ponton, C. B. (2013). Aqueous Electrophoretic Deposition as a Method for Producing an Investment Casting Shell Mould Ceramic Face-Coat. Part 1: Formation of a Carbon-Filled Investment Casting Wax Electrode Material. *Journal of Materials Science*, *48*(21), 7476–7492. doi: 10.1007/s10853-013-7562-8

Roberts, P. B., & Kubasco, A. J. (1982). Centaur Gas Turbine Modification and Development for Solar-Fossil Hybrid Operation. (September).

Rodrigues, T. T., & Link, R. (2012). Effect of the Turbulence Modeling in the Prediction of Heat Transfer in Suction Mufflers.

Rodríguez, E., Arqués, J. L., Rodríguez, R., Nuñez, M., Medina, M., Talarico, T. L., ... Masuelli, M. (1989). We are IntechOpen , the world ' s leading publisher of Open Access books Built by scientists , for scientists TOP 1 %. *Intech*, *32*(tourism), 137–144. Retrieved from https://www.intechopen.com/books/advanced-biometric

-technologies/liveness-detection-in-biometrics

Rogelj, J., Smith, S. M., & Yu, S. (2021). Net-zero emissions targets. , 18–28.

RSA. (2015). Euro IV , Euro V and VI Emissions Regulations for Heavy Duty Vehicle. , *2009*(September 2015), 1–10.

Rubechini, F., Schneider, A., Arnone, A., Dacca, F., Canelli, C., & Garibaldi, P. (2011). Aerodynamic Redesigning of an Industrial Gas Turbine. *Proceedings of ASME Turbo Expo 2011*, 1–8. Retrieved from http://rubechini2011.pdf doi: 10.1115/GT2011-46258

Saidur, R., Hasanuzzaman, M., Sattar, M. A., Masjuki, H. H., Irfan Anjum, M., & Mohiuddin, A. K. M. (2007). An Analysis of Energy Use, Energy Intensity and Emissions at the Industrial Sector of Malaysia. *International Journal of Mechanical and Materials Engineering*, *2*(1), 84–92.

Sakaoglu, S., & Kahveci, H. S. (2019). Effect of turbine blade tip cooling configuration on tip leakage flow and heat transfer. *Proceedings of the ASME Turbo Expo*, *5A-2019*, 1–10. doi: 10.1115/GT2019-90130

Salim, S. M. (2014). Wall y + Strategy for Dealing with Wall-bounded Turbulent Flows. (January 2009).

Sanguesa, J. A., Torres-Sanz, V., Garrido, P., Martinez, F. J., & Marquez-Barja, J. M. (2021). A review on electric vehicles: Technologies and challenges. *Smart Cities*, *4*(1), 372–404. doi: 10.3390/smartcities4010022

Satish, T. N., Murthy, R., & Singh, A. K. (2014). Analysis of Uncertainties in Measurement of Rotor Blade Tip Clearance in Gas Turbine Engine Under Dynamic Condition. *Proceedings of the Institution of Mechanical Engineers, Part G: Journal of Aerospace Engineering*, *228*(5), 652–670. Retrieved from http://www.scopus.com/inward/record.url?eid=2-s2.0-84899069076{\&}partnerID=40{\&}md5=507620baf760f1f31e7012b5ec05f273 doi: 10.1177/0954410013478523

Schmitz, J. T., Perez, E., Morris, S. C., Corke, T. C., Clark, J. P., Koch, P. J., & Puterbaugh, S. L. (2016). Highly Loaded Low-Pressure Turbine: Design, Numerical, and Experimental Analysis. *Journal of Propulsion and Power*, *32*(1), 142–152. Retrieved from http://arc.aiaa.org/doi/10.2514/1.B35334 doi: 10.2514/1.B35334

Schobeiri, M. T., Rezasoltani, M., Lu, K., & Han, J. C. (2014). A Combined Experimental and Numerical Study of the Turbine Blade Tip Film Cooling Effectiveness under Rotation Condition. In *Turbine technical conference and exposition.*

Science, M. (2010). IGCC State-of-the-Art Report. *Science*(April).

Sederberg, T. W. (2016). Computer Aided Geometric Design Course Notes. , 288. Retrieved from https://books.google.com/books?hl=en{\&}lr={\&}id=k7ziBQAAQBAJ{\&}oi=fnd{\&}pg=PP1{\&}dq=computer+aided+geometric+design{\&}ots=BXNt0K1cBD{\&}sig=883sumK0Q1PYE-7k9RUNKDf9Ge8{\%}5Cnhttp://scholarsarchive.byu.edu/facpub/1/

Self, S. J., Reddy, B. V., & Rosen, M. a. (2012). Review of Underground Coal Gasification Technologies and Carbon Capture. *International Journal of Energy and Environmental Engineering*, *3*(1), 16. doi: 10.1186/2251-6832-3-16

Sethunathan, P., Prathap, S., Prabakaran, M., Pawanraj, S., & Siddharth, R. (2007). Design and Analysis of Gas Turbine Internal Cooling Passage. *International Journal of Innovative Research in Science, Engineering and Technology (An ISO Certified Organization)*, *3297*(6), 13533–13539. Retrieved from www.ijirset.com

Sharma, D. K. (2010). Modeling the Steam Gasification Reactions for Reactor Design. *Energy Sources, Part A: Recovery, Utilization, and Environmental Effects*, *33*(1), 57–71. doi: 10.1080/15567030902967819

Sharma, S., Sharma, A., & Sharma, M. (2015). Gas Turbines-Current Scenario

and Future Prospects in India. *International Journal of Scientific & Engineering Research*, *6*(8), 867–876.

Shirzadi, M. R., & Saeidi, H. (2012). The Effects of Tip Clearance on Performance of a Heavy Duty Multi Stages Axial Turbine. *Proceedings of ASME Turbo Expo*(June 11-15), 1–11.

Shuang, L., & Ming, Z. B. (2010). Experimental study on a transpiration cooling thermal protection system. *Science China Technological Sciences*, *53*(10), 2765–2771. doi: 10.1007/s11431-010-4055-8

Sivashanmugam, V. K., Arabnia, M., & Ghaly, W. (2010). Aero-Structural Optimization of an Axial Turbine Stage in Three-Dimensional Flow. In *Asme turbo expo 2010: Power for land, sea and air.*

Siw, S. C., Karaivanov, V. G., Chyu, M. K., Slaughter, W. S., & Alvin, M. A. (2009). Influence of Internal Cooling Configuration on Metal Temperature Distributions of Future Coal-Fuel Based Turbine Airfoils. *Proceedings of the ASME Turbo Expo*, *3*(PART B), 725–736. doi: 10.1115/GT2009-59829

Škrjanc, I., & Klan, G. (2007). Cooperative Collision Avoidance between Multiple Robots Based on Bézier Curves Statement of the Problem Path Planning Based Bernstein-Bézier Curves. , 34–43.

Smolny, A., Blaszczak, J., & Sobczak, K. (2011). Performance Improvement through the Vane Clocking Effect in a Two-Stage Impulse Turbine. *Mechanics and Mechanical Engineering*, *15*(3), 343–354.

Soares, C. (2015). *Gas Turbine Major Components and Modules*. doi: 10.1016/b978-0-12-410461-7.00004-3

Soghe, R. D., Innocenti, L., Andreini, A., & Poncet, S. (2010). Numerical Benchmark of Turbulence Modeling in Gas Turbine Rotor-Stator System. In *Power for land, sea and air* (pp. 771–783). Retrieved from `http://link.aip.org/link/abstract/ASMECP/v2010/i44021/p771/s1` doi: 10.1115/GT2010-22627

Spencer, D. (2019). BP Statistical Review of World Energy Statistical Review of World. *The Editor BP Statistical Review of World Energy*, 1–69. Retrieved from https://www.bp.com/content/dam/bp/business-sites/en/global/corporate/pdfs/energy-economics/statistical-review/bp-stats-review-2019-full-report.pdf

Spliethoff, H. (2010). *Power Generation from Solid Fuels* (Vol. 21). doi: 10.1007/978-3-642-02856-4

Starr, F., & Cormos, C. (2011). Materials Challenges and Gasifier Choices in IGCC Processes for Clean and Efficient Energy Conversion. *Materials Research Innovations*, *15*(6), 428–446. doi: 10.1179/143307511X13189528030870

Stern, F., Wilson, R. V., Coleman, H. W., & Paterson, E. G. (2001). Comprehensive approach to verification and validation of CFD simulations—Part 1: Methodology and procedures. *Journal of Fluids Engineering, Transactions of the ASME*, *123*(4), 793–802. doi: 10.1115/1.1412235

Sunden, B., & Xie, G. (2010). Gas Turbine Blade Tip Heat Transfer and Cooling: A Literature Survey. *Heat Transfer Engineering*, *31*(7), 527–554. Retrieved from http://www.tandfonline.com/action/journalInformation?journalCode=uhte20{\%}7B{\%}25{\%}7D5Cnhttp://dx.doi.org/10.1080/01457630903425320http://www.tandfonline.com/action/journalInformation?journalCode=uhte20{\%}5Cnhttp://dx.doi.org/10.1080/01457630903425320 doi: 10.1080/01457630903425320

Szwaba, R., Kaczynski, P., Doerffer, P., & Telega, J. (2016). Flow Structure and Heat Exchange Analysis in Internal Cooling Channel of Gas Turbine Blade. *Journal of Thermal Science*, *25*(4), 336–341. Retrieved from http://link.springer.com/10.1007/s11630-016-0868-5 doi: 10.1007/s11630-016-0868-5

Tabatabaee, N. S., & Boroomand, M. (2018). Preliminary Design of an Axial Turbine Stage for a Microjet Engine Preliminary Design of an axial turbine stage for a microjet engine. (February 2012).

Takase, M., Kipkoech, R., & Essandoh, P. K. (2021). A comprehensive review of energy scenario and sustainable energy in Kenya. *Fuel Communications*, *7*, 100015. Retrieved from `https://doi.org/10.1016/j.jfueco.2021.100015` doi: 10.1016/j.jfueco.2021.100015

Talya, S. S., Rajadas, J. N., Chattopadhyay, A., Rajadas, J. N., & Multidisciplinary, A. C. (1999). Multidisciplinary Optimization for Gas Turbine Airfoil Design. , *2767*(October). doi: 10.1080/174159700088027731

Theju, V., Uday, P. S., PLV, G. R., & C J, M. (2007). Design and Analysis of Gas Turbine Blade. *International Journal of Innovative Research in Science, Engineering and Technology (An ISO Certified Organization)*, *3297*(6), 13533–13539. Retrieved from `www.ijirset.com`

Thulin, D., Howe, D. C., Singer, I. D., & Group, W. A. (1982). *Energy Efficient engine High-Pressure Turbine Detailed Design Report* (Tech. Rep.).

Timko, L. (1984). *Energy Efficient Engine High Pressure Turbine Component Test Performance Report* (Tech. Rep.).

Timmerman, G. (2014). Approximating Continuous Functions and Curves using Bernstein Polynomials.

Tirgar, R., Sarmazdeh, A. M., Nezhad, M. M., & Tahani, M. (2014). Modelling of Steam Injection Effects on Performance Parameters and NOx Emissions of a Gas Turbine. *J. Appl. Sci. Res.*, *10*(May), 331–336.

Tu, J., Yeoh, G.-H., & Liu, C. (2018). *CFD Solution Analysis: Essentials*. doi: 10.1016/b978-0-08-101127-0.00006-4

U.S Energy Information Administration. (2016). *International Energy Outlook 2016 with Projections to 2040* (Vol. 0484) (No. May). Retrieved from `http://www.eia.gov/forecasts/ieo/world.cfm`

Varge, B., Óvari, G., & Kavas, L. (2016). The Turbine Inlet Temperature and Compressor Pressure Ratio, the Siamese Twins of the Gas Turbine Engines. *Scientific Research and Education in the Air Force*, 393–398. doi: 10.19062/2247-3173.2016.18.1.53

Wang, T., & Gary, S. (2017). *Integrated Gasification Combined Cycle (IGCC) Technologies* (T. Wang & S. Gary, Eds.). Woodhead Publishing.

Weston, K. C. (2000). Energy Conversion - Chapter Five. *Energy Conversion*, 169–223. Retrieved from `http://www.personal.utulsa.edu/{~}kenneth-weston/`

Wiberg, W., & Anton, N. (2013). Aerodynamic design of a gas turbine rotor blade for the KTH test turbine. , 77.

William W. Bathie. (1996). Gas Turbines and Jet Engines. *Fundamentals of gas turbine engines*, 169–223.

Xu, L., Bo, S., Hongde, Y., & Lei, W. (2015). Evolution of Rolls-royce Air-cooled Turbine Blades and Feature Analysis. *Procedia Engineering*, *99*, 1482–1491. Retrieved from `http://www.sciencedirect.com/science/article/pii/S1877705814038065` doi: 10.1016/j.proeng.2014.12.689

Xue, S., & Ng, W. F. (2018). Turbine blade tip external cooling technologies. *Aerospace*, *5*(3), 1–32. doi: 10.3390/aerospace5030090

Xuelei, Z., Songling, W., Haiping, C., & Lanxin, Z. (2010). The Influence of Firing Medium or Low Heat Value Fuel on the Safe Operation of Gas Turbine. (93102802), 1–3.

Yamada, T., & Asako, Y. (2007). Scale Effect on Gaseous Flow Around a Micro-Scaled Gas Turbine Blade. *Heat Transfer Engineering*, *28*(8-9), 696–703. doi: 10.1080/01457630701326357

Yang, D., & Feng, Z. (2007). Tip Leakage Flow and Heat Transfer Predictions for Turbine Blades. *Power for Land, Sea and Air*(May 14-17), 1–8.

Yu, K., Hu, L., Yang, X., & Yue, Z. (2012). Influence of tip injection and

film cooling for blade tip flow and heat transfer. *Applied Mechanics and Materials*, *117-119*, 643–646. doi: 10.4028/www.scientific.net/AMM.117-119.643

Yuri, M., Tsukagoshi, K., Hada, S., Masada, J., & Ito, E. (2013). Development of 1600 C-Class High-efficiency Gas Turbine for Power Generation Applying J-Type Technology. *Mitsubishi Heavy Industries Technical Review*, *50*(3), 1–10. Retrieved from https://www.mhi-global.com/company/technology/review/pdf/e491/e491018.pdf

Zakariyah, S. S. (2014). GAS LAWS & KINETIC. (August 2013). doi: 10.13140/2.1.4809.6965

Zaniewski, D., Klimaszewski, P., Witanowski, L., Jedrzejewski, L., Klonowicz, P., & Lampart, P. (2019). Comparison of an Impulse and a Reaction Turbine Stage for an ORC Power Plant. *Archives of Thermodynamics*, *vol. 40*(No 3), 137–157. doi: 10.24425/ather.2019.129998

Zhalehrajabi, E., Rahmanian, N., & Hasan, N. (2014). Effects of Mesh Grid and Turbulence Models on Heat Transfer Coefficient in a Convergent – Divergent Nozzle. (October 2013), 265–271. doi: 10.1002/apj

Zhang, G., Zhu, R., Xie, G., Li, S., & Sunden, B. (2021). Optimization of cooling structures in gas turbines: A review. *Chinese Journal of Aeronautics*, *35*, 18–46. doi: 10.1016/j.cja.2021.08.029

Zhao, Y., McDonell, V., & Samuelsen, S. (2019). Influence of Hydrogen Addition to Pipeline Natural Gas on the Combustion Performance of a Cooktop Burner. *International Journal of Hydrogen Energy*, *44*(23), 12239–12253. Retrieved from https://doi.org/10.1016/j.ijhydene.2019.03.100 doi: 10.1016/j.ijhydene.2019.03.100

Zheng, Q., Gao, J., & Li, B. (2010). Study of viscous controlled vortex design of a LP turbine stage. *Proceedings of the ASME Turbo Expo*, *7*(PARTS A, B, AND C), 1489–1501. doi: 10.1115/GT2010-23123

Zhou, C., Hodson, H., Tibbott, I., & Stokes, M. (2012). Effects of winglet

geometry on the aerodynamic performance of tip leakage flow in a turbine cascade. *Journal of Turbomachinery*, *135*(3), 1–12. doi: 10.1115/1.4007831

Zikanov, O. (2010). *Essential Computational Fluid Dynamics*. Retrieved from http://scholar.google.com/scholar?hl=en{\&}btnG=Search{\&}q=intitle:No+Title{\#}0{\%}5Cnhttp://books.google.com/books?hl=en{\&}lr={\&}id=e7fR2yu3HvQC{\&}oi=fnd{\&}pg=PR15{\&}dq=Essential+Computational+Fluid+Dynamics{\&}ots=sDyvXTL5tM{\&}sig=-stn0knXqaf03hUjG7b49bavB0I

Zohuri, B. (2015). Combined cycle driven efficiency for next generation nuclear power plants: An innovative design approach. *Combined Cycle Driven Efficiency for Next Generation Nuclear Power Plants: An Innovative Design Approach*, 1–359. doi: 10.1007/978-3-319-15560-9

Zolfagharian, M. M., Rajabi-Zargarabadi, M., Mujumdar, A. S., Valipour, M. S., & Asadollahi, M. (2014). Optimization of Turbine Blade Cooling Using Combined Cooling Techniques. *Engineering Applications of Computational Fluid Mechanics*, *8*(3), 462–475. doi: 10.1080/19942060.2014.11015529